Recent ~~abrupt~~ thermohaline shifts in the Adriatic Sea ~~physical properties~~ and their potential consequences

Elena Terzić[1] and Ivica Vilibić[1,2]

[1]Ruđer Bošković Institute, Division for Marine and Environmental Research, Bijenička cesta 54, 10000 Zagreb, Croatia
[2]Institute for Adriatic Crops and Karst Reclamation, Put Duilova 11, 21000 Split, Croatia

Correspondence: Elena Terzić (eterzic@irb.hr)

Abstract. The Adriatic Sea has ~~recently undergone rapid transitions in its thermohaline properties, affecting the entire water column—from surface layers, influenced by changing atmospheric and hydrological forcings, to the deepest layers, which are increasingly replenished by significantly warmer and saltier waters. The Mediterranean Sea as a whole is warming and salinifying at rates exceeding those of the global ocean and is projected to continue this trend throughout the 21st century. Consequently, the lateral inflow of heat and salt through the Strait of Otranto is modifying the thermohaline structure of the Adriatic Sea. However, available evidence suggests that a substantial portion of these changes arises from locally amplified Adriatic processes, as observed rates are several times higher than those reported forthe Mediterranean at large. This paper reviews the key Adriatic changes documented primarily over the past decade, including shifts in the inflow and properties of inflowing Eastern Mediterranean waters, progressive warming of the northern Adriatic shelf,~~ warmed and salinified rapidly over the past two decades, and the ~~recurrent formation of surface~~ changes are not uniform with depth. We combine 34 306 quality-controlled temperature and salinity casts spanning 1950–2025, from which two climatologies are built, with Argo profiling in the Southern Adriatic Pit, to quantify the vertical structure of the change and to test formally whether it is abrupt. Between the 1950–1999 and 2000–2025 climatologies the southern Adriatic warmed and salinified at every depth and season, by 0.10–0.52 in salinity and up to 1.6 °C in temperature, significantly so once cast clustering within cruises is accounted for. Amplification relative to the Mediterranean is strongly depth-dependent: over 2000–2025, on matched periods and an identical pipeline, southern Adriatic rates exceed the Mediterranean basin median 6.1-fold for temperature and 3.8-fold for salinity at 700–1200 m, but only 0.5–0.7-fold for temperature above 200 m, while surface salinification runs at 4.3 times the basin median. On the northern shelf, which the sampling supports only to 50 m, summer warming reaches 3.0 °C at 20 m. Near-surface salinity maxima (~~so-called~~ "surface saline lakes") ~~,~~ occur in an annual mean of 4.4 % of casts before 2014 and ~~North Adriatic Dense Water cascading increasingly driven by increased salinity at its formation sites. The rates of these changes are quantified, also through a comparison of 21st-century versus 20th-century thermohaline properties, and their potential impacts on regional climate extremes, biogeochemistry, marine ecosystems, fisheries, and aquaculture are discussed~~ 17.1 % after, a factor of 3.9 and a statistically significant level shift, once vertical resolution is controlled for. The intermediate salinity maximum has lost the dominant band of the classical description: 42 % of detected maxima fell within 100–200 m in 1950–1999 against 16 % in 2000–2025, the rest spreading both shallower and deeper, while the share of casts carrying two maxima shows no consistent change. Where two maxima coexist they moved apart, their median separation growing from 92 to 113 m, and

diverged in density, the shallower one becoming 0.12 kg m^{-3} lighter as it salinified while the deeper one stayed close to its isopycnal, so they are not one migrating core. Over 2014–2024 the steric contribution in the Southern Adriatic Pit is negative, -5.4 ± 2.5 mm yr^{-1} over 0–1000 m, because halosteric contraction exceeds thermosteric expansion, so local sea level rise must be mass-driven. Salt fingering has intensified below the classical intermediate core but not within it, driven by a weakening of stratification, so the layers into which the salt has moved are also those newly able to carry it deeper. Consequences for ventilation, biogeochemistry and ecosystems are discussed as hypotheses.

1 Introduction

Coastal ~~ocean regions are known to respond more rapidly~~ and marginal seas respond to climate forcing faster than the open ocean, whether the forcing ~~originates~~ arrives from the atmosphere~~(surface forcing), land (hydrological forcing), or lateral boundaries connecting coastal regions with the open ocean (Holt et al.~~ , ~~2025; Richardson et al., 2025; Wagawa et al., 2025). One of the most extensively studied coastal regions is the Mediterranean Sea (Malanotte-Rizzoli et al., 2014), which—although thousands of kilometres long and up to 5 km deep—exhibits changes at much faster rates than~~ from land, or across lateral boundaries (Holt et al., 2025; Richardson et al., 2025; Wagawa and Igeta, 2025). The Mediterranean Sea is the archetype, changing at rates above the global ocean ~~(Schroeder et al., 2017; Juza et al., 2022). Such changes in the physical systems of coastal seas may have unprecedented consequences for biogeochemical processes, living organisms, and higher trophic levels, including aquaculture and fisheries, which are known to respond to accelerated physical changes (Pairaud et al., 2014; Grbec et al., 2015; Hassoun et al., 2022). Furthermore, feedbacks from the rapidly changing coastal ocean to the atmosphere, land, and hydrosphere may also be amplified (Small et al., 2001; Khodayar and Hoerner, 2020; He et al., 2022), resulting in changes in extremes that may be critical for populations in surrounding areas (Bermúdez et al., 2021).~~

~~A semi-enclosed sea deeply embedded within the European continent and subject to strongly varying boundary forcing is the Adriatic Sea—the northernmost embayment of the Mediterranean Sea , approximately~~ mean (Schroeder et al., 2017; Juza et al., 2022) , and within it the Adriatic Sea is a particularly sensitive sub-basin: semi-enclosed, 800 km long, 200~~km wide,~~ km wide and up to ~~1 230 m deep. The history and longevity of environmental observations in the Adriatic are exceptionally rich, including systematic interdisciplinary field campaigns that began in the early twentieth century (Buljan and Zore-Armanda, 1976; Artegiani et al., 1997; Lipizer et al., 2014; Fortibuoni et al., 2017). Based on both early and modern data, many physical processes that characterize Adriatic dynamics have been documented with increasing understanding over time. These include, among others: (i) the generation of~~ 1230 m deep, strongly influenced by riverine input, and subject to orographically shaped air–sea forcing.

Four Adriatic processes are directly relevant here. North Adriatic Dense Water (NAddW) ~~on the northern Adriatic shelf , which, through density currents, transports dissolved oxygen to deep layers and sustains benthic organisms (Zore-Armanda, 1963; Marini et al. , 2006; Pusceddu et al., 2013; Chiarini et al., 2022a; Vilibić et al., 2023); (ii) decadal-scale modulations of the inflow of ultra-oligotrophic and saline Levantine~~ forms on the shallow northern shelf and cascades along the bottom into the Jabuka and Southern Adriatic Pits, ventilating them (Zore-Armanda, 1963; Marini et al., 2006; Vilibić et al., 2023).

The inflow of saline Levantine and Cretan Intermediate Water (LIW~~; Malanotte-Rizzoli et al., 2003) into the Adriatic (Buljan, 1953; Gačić et al., 2010; Civitarese et al., 2023), which shape~~ /CIW) is modulated on decadal scales by the Adriatic–Ionian Bimodal Oscillating System (Gačić et al., 2010; Civitarese et al., 2023), shaping the nutrient budget ~~and primary production across much~~ of the basin ~~(Civitarese et al. , 2010; Vilibić et al., 2012; Ozer et al., 2022); (iii) open-ocean~~ (Civitarese et al., 2010) . The Eastern Mediterranean Transient of the early 1990s, when the Aegean replaced the Adriatic as the dominant source of eastern Mediterranean deep water (Roether et al., 1996), is the precedent for an abrupt reorganisation on this scale, and it altered Adriatic properties directly (Vilibić et al., 2012). Open-ocean convection in the ~~deep~~ Southern Adriatic Pit ~~(Gačić et al., 2002), which represents a major source of deep waters for~~ supplies deep water to the Eastern Mediterranean ~~(Schlitzer et al. , 1991; Li and Tanhua, 2020); (iv) rapid response timescales and a relatively~~ (Gačić et al., 2002; Schlitzer et al., 1991) . The basin's small internal Rossby radius ~~of deformation compared to the rest of the Mediterranean Sea (Cushman-Roisin and Korotenko, 2007; Kurkin et al., 2020; Pranić et al., 2023), which make the accurate reproduction and forecasting of ocean dynamics extremely challenging, requiring sub-kilometre-scale numerical models; and more~~makes its dynamics fast and spatially fine-grained (Cushman-Roisin and Korotenko, 2007; Pranić et al., 2023).

~~Intuitively, changes in these processes , as well as in the overall characteristics of the Adriatic climate system, may have profound consequences for physical and biogeochemical systems. These impacts occur on top of quasi-monotonous large-scale trends, such as increasing temperature and salinity in the Mediterranean and global oceans (Jordà et al.,~~ Since about 2012 these processes appear to have moved outside their historical envelope. Salinity rose sharply after 2017 ~~; Iona et al.~~(Mihanović et al., 2021; Beg Pa , dense waters formed in 2017, 2018 ~~), declining dissolved oxygen concentrations and biological production (Belgacem et al., 2025; Liu et al., 2025), and other associated changes. The Adriatic Sea, being semi-enclosed and strongly shaped by surrounding orography, may experience these changes more dramatically than more open coastal ocean regions. For example, rising ocean temperatures are driving northward species migration (Moraitis et al., 2019; Shlesinger et al., 2024), reducing available marine habitats (Jordà et al.~~ and 2022 were produced by weak cooling of very saline water rather than by strong cooling (Terzić et al., 2025a; Amorim et al., 2024; Le Meur et al., 2025), and near-surface salinity maxima were documented for the first time (Terzić et al., 2025b). Whether these are genuinely abrupt departures, or the visible part of a gradual trend sampled by a rapidly improving observing system, has not been tested formally. That distinction is important because the observing system changed at almost exactly the time the signal appeared: Argo entered the Adriatic in 2009 and now dominates the deep record (Tintoré et al., 2019).

Three developments make a quantitative reassessment timely. The Adriatic in situ record has been consolidated across archives, so historical shipborne casts and modern autonomous profiles can be processed through a single pipeline. Argo now provides more than a decade of deep profiling in the Southern Adriatic Pit, ~~2020), and triggering mass mortality events (Rivetti et al. , 2014). In the Adriatic , species are constrained by geography and cannot migrate beyond the northern basin. Consequently, some cold-water species—particularly those inhabiting deep accumulation areas (e.g., the Jabuka Pit)—may face local extinction, as their adaptive capacity might be lower than the rate of ongoing climate change (Carlot et al. , 2025). Beyond living organisms, other impacts of locally amplified changes may exceed the adaptive capacity of coupled human–natural systems, including coastal resilience to sea level rise and flash flooding (Mattei et al., 2025; Khodayar et al., 2025), as well as~~

the sustainability of local food resources, fisheries, and agriculture (Olschewski et al. , 2024). enough to resolve the vertical structure of the change rather than only its surface expression. The same pipeline can also be applied to every Mediterranean sub-basin, which turns the recurring claim of local amplification from a qualitative impression into a testable ratio.

This article presents a selection of physical processes in the Adriatic Sea that have been locally amplified or substantially altered over the past decade, based on comparisons between recent observations and historical records spanning many decades to over a century. These include changes in thermohaline circulation and the hydrological cycle, salinization of shelf regions, and a paradigmatic shift in key processes such as dense water formation and cascading. An assessment of the multi-decadal dataset and eventual biases coming from time-space inhomogeneity are discussed first in Section2, followed by presentation of selected processes in Section 3. research article is organised as follows. Section 2 describes the observational dataset and the methods. Section 3 addresses four questions: how large are the Adriatic changes, and are they distinguishable from sampling variability (Sects. 3.1–3.2)? Is the amplification relative to the Mediterranean general, or confined to particular depths (Sect. 3.3)? Did the vertical distribution of salinity in the intermediate layer change over time (Sect. 3.4)? Is the increase in near-surface salinity maxima (surface saline lakes) an abrupt shift or an artefact of vertical resolution (Sect. 3.5)? Sections 3.6–3.7 quantify the steric and double-diffusive consequences. All results in Sect. 3 are new analyses performed for this paper. Section 4 subsequently discusses some potential consequences of these changes, including impacts on water density and sea level, the statistics of climate extremes, biogeochemical cycling, and marine biodiversity, as well as implications for species migration, fisheries, and aquaculture. In this way, directions for future research are outlined, ranging from analyses of fundamental physical changes(e.g., circulation and thermohaline variability) to their broader environmental and societal impacts. discusses the implications as hypotheses and identifies the observations and model experiments that would test them.

2 Data and methods

Temperature and salinity time series in the Adriatic Sea are among the longest in the world's coastal seas, with systematic basin-scale observations dating back to the 1910s (Vilibić et al., 2023). Unfortunately, the First World War interrupted data collection, which resumed only after the Second World War.At the Palagruža Sill transect in the middle Adriatic, the first systematic observations were initiated in 1952 (Buljan and Zore-Armanda, 1966, 1979; Zore-Armanda et al., 1991)and have since been conducted on a seasonal to monthly basis up to the present day. Nevertheless, sampling procedures and instrumentation have changed over time, raising questions about the homogeneity and long-term reliability of the multidecadal thermohaline records and the possible presence of sampling-related biases.

2.1 Observational dataset

In the analyses presented in Section 3, climatologies were constructed using all available Climatologies are built from all quality-controlled in situ temperature and salinity observations collected during the periods casts available in the Adriatic for 1950–1999 (20th century) and 2000–2019 (21st century). The dataset was compiled from several sources: (1) the and 2000–2025. Three archives are combined. The SeaDataNet Pan-European infrastructure (https://www.seadatanet.org)supplies

the Mediterranean aggregated dataset SDC_MED_DATA_TS_V2 (Simoncelli et al., 2020), which archives ~~Mediterranean observations up~~ observations from 1912 to 2019~~; (2) local Adriatic databases , primarily maintained~~ , retrieved in December 2025. Local Adriatic databases are contributed by the Institute of Oceanography and Fisheries ~~and the Rudj er Bošković Institute , with the latest data collected at the end of 2017; and (3)Argo profiling float observations collected in the Mediterranean since 2001 through~~ (Adriatic database 1987–2019, and the Palagruža Sill transect 1952–2018) and the Ruđer Bošković Institute (northern Adriatic transect 1979–2018), together with the Croatian MSFD monitoring CTD set (2019–2023). Argo profiles come from Euro-Argo ERIC~~(https://www.euro-argo.eu), with measurements in the Adriatic beginning in 2009. Prior to 1950, only sparse thermohaline observations were available (Buljan and Zore-Armanda, 1976; Artegiani et al., 1997; Lipizer et al., 2014), while CTD campaigns conducted after 2019 have not yet been systematically archived in a centralized database. Consequently, the post-2019 period—during which the most rapid increases in temperature and salinity were observed (Terzić et al.~~, ~~2025a)—is not included in these climatologies.~~

~~The data were systematically quality controlled during~~ accessed through `argopy` (Maze and Balem, 2020) and retrieved in January 2026; the first Adriatic profile dates from 2009. The Adriatic casts used here are the Adriatic subset of the Mediterranean-wide multiplatform dataset assembled and described by Terzić and Vilibić (2026c), processed through the same chain, so the Adriatic and Mediterranean sides of the comparison in Sect. 2.4 rest on one dataset rather than on two independently curated ones. The cleaned Adriatic in situ files are archived by Terzić and Vilibić (2026a) and the processing and ~~archiving of SeaDataNet observations (SeaDataNet, 2010) and through the~~ analysis code by Terzić and Vilibić (2026b).

Table 1 reports retained cast counts by source, region, period, season and maximum depth. These are the counts entering Figs. 1–2, not the raw archive totals. Quality control follows the originating infrastructure: SeaDataNet procedures (SeaDataNet, 2010) and Argo delayed-mode ~~quality control procedures applied to Argo observations (Wong et al., 2023). For the Palagruža Sill transect dataset, additional quality-control procedures were implemented during previous analyses (e.g., Mihanović et al., 2015, and references therein), resulting in a homogeneous climatological dataset. The remaining Adriatic observations, originating from numerous national (primarily Croatian and Italian) and international research cruises ,~~ procedures (Wong et al., 2023) , with only flags 1 and 2 accepted in both. Casts from national and international cruises outside those archives were quality controlled following SeaDataNet procedures during the assessment ~~of the kilometre-scale Adriatic atmosphere–ocean model described by Pranić et al. (2021)~~described by Pranić et al. (2023). Duplicates are removed by matching position, time and platform before pooling, so a cast archived in more than one source is counted once.

~~The analyses were conducted using the original observational dataset, although one may argue that ocean reanalysis products could provide a more homogeneous time–space coverage.However, the study period spans both the pre-satellite and satellite eras, during which the assimilation of sea surface temperature and sea level anomalies evolved substantially over time. Furthermore, the Argo programme was initiated in the Mediterranean Sea in the early 2000s (Poulain et al., 2007), whereas the first Argo profile in the Adriatic Sea was obtained only in 2009. Such abrupt changes in the availability of deep observations may introduce artificial shifts and trends in deep Adriatic thermohaline properties due to changes in data assimilation constraints (E.Terzić, unpublished results). Similar issues have also been recognized in Mediterranean reanalysis products (Escudier et al. , 2021; Wang et al., 2023). In addition, ocean reanalyses tend to smooth the intensity of the thermocline and pycnocline~~

in the upper ocean (Adani et al., 2011), which may limit their applicability for resolving strongly stratified events such as surface saline lakes (Terzić et al., 2025b). In the present approach, temporal and spatial averaging was applied to minimize sampling-related biases. Such biases are expected to be relatively small in the deep Adriatic, where observations are quasi-uniformly distributed among different in situ platforms (Fig. All analyses use the record to 2025. The climatological comparison — Figs. 1, 2 and 4 and Tables 1). However, some biases may remain embedded in the climatologies for shallow regions such as the northern Adriatic, particularly for salinity, owing to pronounced east–west gradients driven by freshwater discharges (Artegiani et al., 1997). and 2 — contrasts 1950–1999 with 2000–2025, and the 34 306 casts of Table 1 are drawn from those two windows.

The two periods are not sampled alike. Argo supplies 44.3 % of the 21st-century southern Adriatic casts and none of the 20th-century ones, and Argo profiles do not reach the top few metres – their median first sampled depth in the southern Adriatic is 5.5 m, against 2.8 m for the 21st-century casts of all platforms together – so the shallowest bins are the least comparable between periods (Sect. 3.1).

Following the multi-decadal and even centennial trends observed in the Mediterranean, Adriatic Sea temperature and salinity have also been found to steadily increase over the last century, exhibiting strong interannual to basin-wide decadal variability. This variability is driven by oscillatory processes in the northern Ionian Sea (i.e.,

2.2 Regions, binning and climatologies

The northern and southern Adriatic are delimited by two polygons, labelled DJ1 and DJ3 after the Mediterranean sub-basin nomenclature of Manca et al. (2004). The labels follow that nomenclature but the boundaries do not: rather than straight lines of latitude, they follow the coastline and the Adriatic–Ionian Bimodal Oscillating System, BiOS; Gačić et al., 2010; Batistić et al., 2014; Civitarese et al., 2023) and by changes in the surface heat budget associated with the Atlantic Multidecadal Oscillation (Mariotti and Dell'Aquila, 2012; Macias et al., 2013). Up to the end of the 20th century, these increases were largely modulated and therefore partially insignificant across large parts of the Adriatic, with trends not exceeding the magnitude of observed variability (Lipizer et al., 2014). Consequently, Adriatic water mass climatology was considered preserved in terms of source characteristics, within uncertainties related to natural variability and samplingbias (Vilibić bathymetry, so that the northern shelf is separated from the middle Adriatic along the Zadar–Ancona axis rather than across it, and Orlić, 2001). However, this situation has changed over the last decade, with the most prominent emerging changes described in the following subsections. the southern Adriatic is separated from the middle along the Gargano–Pelješac axis. Bounding boxes are given in Table 1 and the polygon files are archived with the analysis code. Seasons are three-month bins, JFM, AMJ, JAS and OND. Casts are binned onto 22 standard levels between 5 and 1200 m. A cast contributes to a level only where it carries a finite, flag-1 or flag-2 value; no vertical interpolation across gaps is performed, and casts that do not reach the full depth simply stop contributing below their deepest level. A level is retained when at least 5 % of the casts in that region, period and season reach it. Averaging is by measurement within each level, and a second pass rejects values more than one standard deviation from the first-pass bin mean.

Temperature and salinity are binned as measured, that is as in situ temperature and practical salinity; practical salinity is a ratio and is therefore reported without units. Potential density anomaly referenced to the surface (σ_0) is derived from them through TEOS-10 (IOC et al., 2010), which converts practical salinity to absolute salinity and in situ to conservative temperature internally, using the `gsw` implementation. The Argo-based analyses of Sects. 2.7 and 2.8 work directly in absolute salinity and conservative temperature, since they require the thermodynamic coefficients. The binning and pooling procedure is described in more detail by Terzić and Vilibić (2026c), who apply it Mediterranean-wide.

~~A strong increase in salinity in the Adriatic Sea was initially observed in 2017, a half-decade after a centennial dense water generation event in~~

2.3 Uncertainty of climatological differences

Counting casts as independent measurements would overstate how much information the climatologies contain. A research cruise typically occupies a region for a few days and takes many casts in that time, so those casts largely repeat one synoptic state rather than sampling the climate independently: 200 casts from four cruises carry far less information than 200 casts taken on 200 separate occasions.

The uncertainty is therefore estimated by bootstrapping. No values are simulated and no distribution is assumed: each of the 2000 replicate datasets is built only from observations already in the archive, drawn at random with replacement, so a given cast may appear several times in one replicate and not at all in another. The period mean is recomputed on each replicate, and the confidence interval is the spread of those 2000 means. The wider they scatter, the less the single observed mean can be relied on.

The resampling unit is the cruise-day rather than the cast: all casts taken by one cruise on one day enter or leave a replicate together, so the replicates inherit the repetition of the real sampling. The ratio between the variance obtained this way and the variance obtained by treating casts as independent is the variance inflation factor, which is at least one, so clustering always widens the interval: a value of 6 means the casts carry the information of about one sixth as many independent observations. For 2000–2025 it is 1.8–2.2 in the southern Adriatic and 5.7–6.3 in the northern Adriatic ~~in 2012 (Mihanović et al., 2013), which was so strong to rapidly affect the BiOS regime in the northern Ionian Sea (Gačić et al., 2014). 2017 was particularly dry year, during which salinity maxima was for the first time documented at the surface. The maxima have been driven by high evaporation, low vertical mixing (weaker winds) and lower-than average river discharges (Mihanović et al., 2021; see details in Section 3.3). Such conditions had been very rarely observed previously, even in~~ (for 1950–1999, when sampling was still more cruise-bound, 3.8–5.7 and 7.0–8.3), so the ~~well-surveyed Palagruža Sill transect (e.g., during strong Adriatic 'ingressions', i.e., Zore-Armanda, 1991; Zore-Armanda et al.~~ northern shelf, where cruises are denser and more repetitive, is far more strongly clustered. Shaded envelopes in Figs. 1–2 are 95 % confidence intervals on the period mean at each level, computed this way; they are not standard deviations.

Northern Adriatic results are reported only to 50 m, because below that depth the region is barely sampled: 905 casts reach beyond 50 m in 2000–2025 against 12 697 above it, over 90 % of those stop between 50 and 75 m, and fewer than 30 reach

100 m in either period (Table 1), ~~1991; Artegiani et al.~~ so the 50–200 m row of that table describes a layer that is in practice 50–75 m thick.

2.4 Adriatic–Mediterranean rate comparison

To make the amplification claim quantitative, deseasoned linear trends per decade are computed for every Mediterranean sub-basin with the same pipeline, bins, quality control and estimator as for the Adriatic, so that the only difference between the two sides of the comparison is the ocean rather than the method. The monthly basin-by-depth series and the seasonal-harmonic trend model are those of Terzić and Vilibić (2026c), re-fitted here over the matched window. Mediterranean values are the median across basins outside the Adriatic with the interquartile range; Adriatic values are the median across depth bins within a layer. The Adriatic sub-basins are excluded from the reference median so that the basin is not compared partly against itself; including them changes no ratio qualitatively (the largest effect is on surface salinity, 4.3 to 3.6). The four layers – 5–50, 75–200, ~~1997). In 2017, salinity exceeded 39.0 over most of the surface layer of the Southern Adriatic Pit (SAP) between late spring and mid-autumn, including most of the Palagruža Sill transect (Mihanović et al., 2021). The consequences for the biogeochemical cycles were also considerable, as bacterial abundances in coastal eastern Adriatic regions departed from average values by several standard deviations (Beg-Paklar et al. , 2020). Several other notable thermohaline features were found to precede such conditions, including the occurrence of double salinity maxima, of which the upper and stronger maximum was located at relatively shallow depths (50–200 m; Lučić et al. , 2017; Kokkini et al., 2020). Indeed, the depth of this maximum, associated with the inflow of LIW and Cretan Intermediate Water (CIW; Schroeder et al., 2024) , decreased significantly. Furthermore, salinity at this maximum increased continuously, reaching values exceeding 38.9 over most of the deep southern Adriatic (see, e.g., Argo profiling float data available in near real-time from the Euro-ARGO ERIC data portal, https://dataselection. euro-argo.eu/, last accessed 27 May 2026). The spreading of these saline waters towards deep layers has been facilitated both (1) by enhanced salt fingering and weakened stratification from intermediate to deep layers (Amorim et al., 2024; Terzić et al. , 2025a),~~ 250–600 and ~~(2) dense water cascading from the northern Adriatic that rapidly change near-bottom thermohaline properties in the whole deep Adriatic (see more in Section 3.4).~~

~~When comparing thermohaline climatologies of~~ 700–1200 m – separate the seasonally mixed surface layer, the layer between the seasonal thermocline and the ~~21st and 20th centuries (Fig.1),~~ LIW/CIW horizon, the ~~increase in SAP salinity is clearly evident. Salinity in~~ intermediate-water core, and the deep layers renewed episodically by cascading. The conclusions do not depend on these boundaries, since any partition of the ~~21st century increased quasi-uniformly by approximately 0.10–0.15 at depths below 150 m~~ standard levels gives a temperature ratio below one above 200 m and above four below 700 m. The window is 2000–2025, matching the climatologies; the resulting sampling asymmetry is quantified in Sect. 2.1.

2.5 Change-point analysis

Whether the change in the occurrence of surface saline lakes (SSLs) is a step rather than a gradual drift is tested with the rank-based Pettitt (1979) test. The test tries every possible break year in turn, measures how different the years before it are

from the years after it, and keeps the year that separates them best. Because it searches the years itself, the result is not biased by our picking a year by eye.

Its p-value is obtained by simulation rather than from the standard formula, which assumes each year is independent of the last. We generate 5000 artificial series that match the observed mean, variance and year-to-year correlation but contain no change point by construction, run the identical test on each, and report the fraction that produce a step at least as large as the observed one. Years with fewer than 20 casts are dropped.

Detection of an SSL depends strongly on vertical resolution (Sect. 3.5), so the test is run on a resolution-matched subset: casts with median level spacing ≤ 5 m and at least 8 levels in 0–100 m. The justification is a direct degradation experiment, in which Argo profiles are re-sampled onto progressively coarser grids and the identical detection is repeated (Fig. ~~1), while the increase was largest in the surface and subsurface layers, averaging up to 0.4. This increase may be attributed to more frequent formation of surface saline lakes (see Section 3.3) and to the shoaling of the LIW/CIW inflow, from approximately 200–400 m to 50–150 m~~ A1). ~~This pronounced shoaling is presumably driven by several observed features~~

2.6 Detection of surface saline lakes

Detection uses raw profiles rather than the binned climatologies of Sect. 2.2, so the cast set is assembled separately and is larger: 11 106 southern Adriatic casts over 1950–2025. Occurrence is shown from 1985 because nothing earlier can be evaluated: of the 313 casts from 1950–1984 whose vertical resolution can be computed, not one meets the resolution criteria of Sect. 2.5. The reason is not spacing alone. The gate itself requires 5 m spacing, but even against a looser 10 m criterion no cast before 1975 qualifies; the late 1970s are better sampled than that suggests – 68 % of the 1975–1979 casts meet 10 m and 12 % meet 5 m – and those finer casts fail instead on level count, carrying only three or four levels in the upper 100 m against the eight the detection requires (Fig. A1).

Following Terzić et al. (2025b), a cast is recorded as an SSL when all four of the following hold, with salinity throughout taken as practical salinity and its gradient therefore in m^{-1}: (i) ~~weakening of vertical mixing in the Adriatic Sea due to enhanced stratification and reduced wind forcing (Pomaro et al., 2018; da Costa et al., 2023) , which promotes a shallower salinity maximum; and (ii) the spreading of LIW/CIW at shallower depths in the Levantine, Aegean, and Ionian Seas, with these waters subsequently entering the Adriatic through the Strait of Otranto (Kubin et al. , 2019; Fach et al. , 2021). The latter mechanism has been documented in numerous studies, as significant changes in heat and mass budgets at the LIW/CIW source regions have led to strong salinification of the entire eastern Mediterranean over the past decade (Skliris et al., 2025)~~the vertical salinity gradient falls below $-0.01\ \mathrm{m}^{-1}$ somewhere in 0–100 m, defining a halocline core, chosen among candidates as the one nearest 100 m; (ii) the maximum salinity gradient above the core stays below $0.02\ \mathrm{m}^{-1}$, so the feature is not simply the lower flank of a shallower feature; (iii) the surface is at least 0.05 saltier than the core; and (iv) the water column above the core is statically stable in density, verified with a stratification index computed across the halocline with a 5 m vertical offset, so the salinity inversion is temperature-compensated rather than convectively unstable. Casts with fewer than 8 finite levels in the 0–100 m window are not evaluated.

2.7 Detection of double salinity maxima

The intermediate salinity structure is characterised by locating every prominent subsurface maximum in each cast rather than a single core depth, so that a cast carrying two maxima is described by two, and any change in their separation is measurable. Maxima are found by peak prominence in salinity, the prominence of a peak being the drop in salinity from it to the lowest point that must be crossed to reach any higher peak. The threshold is 0.010. It is set from the data: in casts that carry two maxima the weaker of the two stands 0.021 in salinity above the minimum separating it from the stronger (Sect. 3.4), so a threshold at about half that value admits the real second maximum while rejecting smaller wiggles. It is varied between 0.005 and 0.030 in the sensitivity test of Appendix A (Fig. A3). ~~These increasingly saline waters then propagate into the Adriatic (and other basins; Mallil et al., 2022), rapidly altering its thermohaline and biogeochemical properties there.~~ The search runs to 900 m and requires at least 8 levels in it, a floor that sets aside 469 of the 5761 southern Adriatic casts (8.2 %) as too coarse to carry the detection. The upper 20 m are excluded, so that the near-surface maximum of a surface saline lake is not counted as an intermediate core.

~~Figure 1. Seasonal profiles of temperature, salinity and potential density anomaly (PDA) in the 21st and the 20th century in the southern Adriatic (also referred as the Mediterranean region DJ3 by Manca et al. , 2004) constructed using all available in situ data sources. Right column visualises spatial distributions of the data (SDN stands for SeaDataNet) and data statistics (bottom right): mean (rectangles), median (circles) and range in data casts (vertical lines), with full and empty/dashed symbols and lines for 21st~~ Within each cast, only the two most prominent maxima are retained; no cast is excluded. This guards against a small number of very finely resolved historical profiles whose fine structure is instrumental noise rather than signal: they return up to 268 nominal maxima each, and uncapped, 20 such casts would supply 56 % of all 1950–1999 detections. The cap falls on a similar share of casts in each period, 47 % against 46 %, so it does not favour either. Prominence ranks the maxima because it measures how far a peak stands above the profile around it, and so how much of a distinct feature rather than a ripple it is.

Both choices, together with the prominence threshold itself and the depth a cast must reach, are free parameters, so the whole analysis is repeated across a grid of them in Appendix A (Fig. A3). Both quantities the paper draws conclusions from – how strongly the maxima concentrate in the historical 100–200 m band, and ~~20th century, respectively~~the contrast between how the two members changed in density – hold in every configuration tested.

~~As the eastern Mediterranean has experienced substantial warming in recent decades (Kubin et al. , 2023), LIW/CIW cores entering the Adriatic Sea are also characterized by markedly higher temperatures, reaching up to 1.5 °C in subsurface layers of the southern Adriatic during summer (Fig.1). Note that average temperatures may decrease at the very surface (0 m) in the 21st century; however, this may resultfrom a sampling bias associated with different data types and spatial data distributions. For example, Argo floats normally do not measure at the exact surface (the first bin is typically a few metres below the surface). The intensified increase in near-surface heat content is not unexpected, as surface layer warming has been amplified by the Atlantic Multidecadal Oscillation over the past four decades (Vilibić et al. , 2019; Pastor et al. , 2020; Pisano et al. , 2020). Because these cores are now shallower, LIW temperatures in the Adriatic are influenced by both lateral heat advection from~~

the Ionian Sea and direct heating of the upper portions of this layer, which are now located within the euphotic zone (Buljan and Zore-Armanda, 1976)Each maximum carries its depth, salinity, temperature and σ_0. The σ_0 is what separates the two ways a maximum can move: if it changes depth but keeps its density, the water has simply been displaced; if its density changes as well, the water itself is different. The search runs to 900 m, but frequency statistics use only casts reaching 700 m, since a shallower cast cannot be counted as lacking a deep maximum it could not have seen. Detection runs on the profiles at their native vertical resolution; because that resolution improves over the record, the whole detection is repeated on modern profiles degraded to historical standard depths, and both results are reported in Sect. 3.4. The two periods compared are 1950–1999 and 2000–2025, as for the climatologies.

2.8 Steric decomposition

Thermosteric and halosteric height are computed from ascending Argo profiles reaching at least 1000 dbar in the Southern Adriatic Pit, following Wang et al. (2017), as

$$\mathrm{TSLA} = \int \alpha\,\Theta'\,\mathrm{d}z, \qquad \mathrm{HSLA} = -\int \beta\,S'_{\mathrm{A}}\,\mathrm{d}z, \tag{1}$$

where primes denote anomalies about the period-mean profile and α, β are the TEOS-10 thermal expansion and haline contraction coefficients. The anomaly form is required rather than merely preferred: integrating $\alpha\Theta$ instead of $\alpha\Theta'$ makes the result, and its trend, depend on the temperature scale used, because Θ is measured from an arbitrary origin while α varies with depth. Anomalies remove that origin.

Profiles are interpolated onto a common 0–1000 dbar grid at 5 dbar spacing, the shallowest observation being carried to the surface since Argo does not sample the top few metres (median first sampled depth 5.5 m for the southern Adriatic floats). Monthly means are formed and the annual and semi-annual harmonics removed, and trends are least-squares fits.

Two features of the series govern how it is treated. First, successive months are correlated, so the record carries less information than its 121 monthly values suggest; the confidence intervals therefore rest on an effective sample size, reduced in proportion to the lag-one correlation of the residuals (Bretherton et al., 1999). That correlation is 0.7–0.8, leaving an effective 10–21 independent values, so the intervals are correspondingly wide. Second, the thermosteric and halosteric components move in opposition, and much of what makes each uncertain affects both in the same way and cancels in their sum. Adding two separately fitted trends would discard that cancellation and inflate the uncertainty on the net, so the net is formed profile by profile and trended once. Seventeen floats contribute 694 profiles over April 2010 – September 2025; WMO identifiers are listed in Table 4. Two further floats, 6903805 and 6901865, are excluded because their profiles do not reach 1000 dbar in the Southern Adriatic Pit.

2.9 Double-diffusive diagnostics

Two quantities are distinguished. The Turner angle determines whether the column is in the salt-finger regime ($45° \le \mathrm{Tu} < 90°$); the density ratio R_ρ determines whether fingering there is dynamically effective. They are computed from vertical gradients of

conservative temperature and absolute salinity as

$$\mathrm{Tu} = \arctan \frac{\alpha\,\partial_z \Theta - \beta\,\partial_z S_\mathrm{A}}{\alpha\,\partial_z \Theta + \beta\,\partial_z S_\mathrm{A}}, \qquad R_\rho = \frac{\alpha\,\partial_z \Theta}{\beta\,\partial_z S_\mathrm{A}}, \tag{2}$$

with the four-quadrant arctangent, alongside the squared buoyancy frequency $N^2 = -(g/\rho)\,\partial\rho/\partial z$, which measures how strongly the column is stratified. All are evaluated with the `gsw` implementation of TEOS-10 (IOC et al., 2010). Fingers transport appreciably for $R_\rho < 2$, marginally to about 4, and negligibly beyond about 10 (Schmitt, 1994), because they transport salt only if they reach full amplitude before internal-wave shear disrupts them, and the time they need to grow is set by R_ρ (Kunze, 1987). A column can therefore be entirely finger-favourable by the Turner angle and still transport nothing, so extent and vigour are reported separately. Both use the same 694 Argo profiles as the steric decomposition, a Southern Adriatic Pit set retrieved separately in September 2025, and, like it, need vertical gradients resolved over a few metres through the full column and repeated through the year; only Argo provides that here, so neither can be extended into the shipborne record.

They are evaluated in three layers, because the layers behave differently and averaging across them cancels their changes out. The layers are the ones used throughout: 200–400 m, the classical range of the LIW salinity maximum (Artegiani et al., 1997) and the range within which our detected maxima sit (Sect. 3.4); ~~Kovač et al., 2018; Ozer et al. , 2022). Consequently, nutrients supplied by LIW/CIW to the Adriatic (Marasović et al., 1995; Civitarese et al., 2010; Ljubimir et al.,~~ 400–600 m, into which the deeper maximum has descended; and 600–1000 m, the deep layer. A fourth, 350–550 m, is computed only for comparison with the EMSO-E2M3A mooring in Sect. 4.2 and carries no result here. Profiles are compared before and from 2017 ~~) may be partially consumed before entering the basin, potentially altering the Adriatic Sea's biogeochemical balance. Such trends are following globally observed climate-driven strengthening and redistribution of upper-ocean stratification that alters the depth and structure of the nitracline and phosphacline, changing upper-ocean nutrient availability and biological utilization (Gerace et al., 2025).~~ with a two-sided Mann–Whitney test on the per-profile layer statistics.

~~At depths below 200 m, the temperature in the southern Adriatic is increasing steadily between the 21st and 20th centuries across seasons, and equals 0.4–0.6 °C~~

3 Results

3.1 Southern Adriatic warming and salinification

Between the 1950–1999 and 2000–2025 climatologies the southern Adriatic (DJ3) is warmer and saltier at every depth from 5 to 1200 m and in every season (Fig. 1). ~~Such an increase indicates thorough and quasi-uniform warming of~~ Salinity differences range from $+0.098$ to $+0.522$ and are distinguishable from sampling variability at all 88 depth–season combinations after cruise-day clustering is accounted for. Temperature differences range from -1.22 to $+1.56\,^\circ$C and are significant at 97 % of combinations. The summer of 1950–1999 is the thinnest cell of the whole design, 444 casts against 1852 in 2000–2025 (Table 1), so the summer differences carry the widest intervals and are the ones most exposed to the sampling change discussed next.

The most negative of those differences, −1.22 °C in the entire deep Adriatic, which was already documented in 5 m summer bin, is an artefact of how the surface is sampled rather than a cooling. In summer 1950–1999, 82 % of southern Adriatic casts began at or above 1 m and the median first sample was at the surface; over 2000–2025 only 20 % do, the median first sample is at 2.5 m, and Argo – which supplies most recent profiles – has a median summer first sample at 5.8 m. Binning does not remove this bias, because recent casts enter the shallowest bin only through its deeper, colder part. Against the 20th-century summer thermocline of 0.34 °C m^{-1} over the top 20 m, a first sample at 2.5 m instead of the surface reads about 0.8 °C too cold and one at 5.8 m about 2.0 °C too cold, so the observed −1.22 °C lies between these values. We therefore do not interpret the uppermost summer bin, and read the 5–10 m levels with the 20th century (Lipizer et al., 2014), accelerated at the turn of the century, and intensified in deep layers over the past decade (Terzić et al. , 2025a). Interestingly, density does not change substantially in deep layers (below 600 m , same caution. Below 30 m, where the profile is smooth and the platforms overlap, the differences are positive at every level and season. Below 200 m the warming is 0.4–0.6 °C and quasi-uniform across seasons (Fig.1), as temperature-induced lightening is fully compensated by salinity-induced densification. However, in the 21st century, thermosteric expansion is much stronger than halosteric contraction at subsurface and intermediate depths (20–400 m, Terzić et al. , 2025a), reaching a maximum at the LIW/CIW core (density decrease of approximately 0.2 kg m-3). Over the entire water column, density has been found to decrease on average, consistent with climate projections for the Adriatic and potentially contributing to future sea level rise (Sannino et al., 2022 1, bottom row).

Potential density is the weaker signal: 64 % of depth–season combinations show a significant difference, because thermal and haline effects oppose one another. Below 600 m they compensate almost exactly, which is the physical statement behind the near-zero deep steric trend in Sect. 3.6.

A long (several decades) time ago, the northern Adriatic shelf, being under strong impact of large rivers—primarily of the largest Adriatic river, Po River, draining one third of riverine freshwaters into the Adriatic (Raicich, 1996; Janeković et al. , 2014)—has been recognized as an eutrophic area in which primary production is driven by large nutrient load (Degobbis and Gilmartin, 1990; Franco and Michelato, 1992; Degobbis et al., 2000; Solidoro et al., 2009) . Due to heavy freshwater load, seasonal salinity changes were quite large, with higher values during winterin which horizontal/barotropic processes were dominant, while thermally-driven stratification favours off shore spreading of freshwaters towards the eastern coastline during warm part of a year (Kourafalou, 1999). For that reason, salinity in the eastern section of the northern Adriatic (off the city of Rovinj) ranged in the 20th century from 36.5±2.0 during summer to 37.8pm0.3 during wintertime (Supić et al., 2004), while bottom salinity was quasi-steady and hitting values around (37.6-37.8)pm (0.3-0.4) throughout a year. The latter has been the result of

3.2 Northern Adriatic shelf

In the northern Adriatic (DJ1, Fig. 2, 0–50 m) warming reaches 3.0 °C at 20 m in summer, and surface salinity increases in every season, by +0.09 to +0.18 in winter, spring and autumn but by +1.00 in summer, so the seasonal contrast between the fresh summer surface and the winter state is much reduced (Fig. 2). The evidence is weaker than in the south, and unevenly so: once clustering is accounted for, 88 % of the depth–season combinations reported here are significant for temperature but

only 71 % for salinity. The northern shelf is where the clustering correction is largest, with variance inflation factors of 5.7–6.3, and it is also where 20th-century sampling is concentrated along the western coastline while salinity is systematically higher along the eastern one (Artegiani et al., 1997; Vilibić et al., 2019). The 21st-century casts sit farther east and north than the 20th-century ones (median cast longitude 13.7°E against 13.1°E), on the saltier side of that gradient, so the spatial sampling shift inflates rather than damps the apparent salinification. Northern Adriatic salinity differences should therefore be read as indicative upper bounds rather than established values, and we do not report DJ1 below 50 m at all (Sect. 2.3).

3.3 The amplification is depth-dependent

On matched periods and an identical pipeline (Table 2), the southern Adriatic exceeds the Mediterranean basin median by a factor of 6.1 for temperature and 3.8 for salinity at 700–1200 m. Above 200 m the temperature ratio is 0.5–0.7: the southern Adriatic warms more slowly than the Mediterranean median in the upper layers. Amplification is therefore not a single number: a single figure for the basin would average a sixfold deep signal against an upper-layer deficit and obscure both.

The ratio is one of rates fitted within the 2000–2025 window (Sect. 2.4), not of the climatological differences shown in Figs. 1–2. The changing platform mix still acts inside that window, since Argo's share grows through the 2000s and moves the shallowest sampled depth downward, so the affected bins are tested directly. Restricting the surface layer to 10–50 m, 20–50 m or 30–50 m, which progressively removes the shallowest bins, the ~~inflow of more saline waters from the middle Adriatic~~ 5 m bin among them being the one Argo does not reach, moves the temperature ratio from 0.55 to 0.38, ~~which partially took their path inside the shelf (Orlić et al.~~0.37 and 0.35 and the salinity ratio from 4.3 to 4.1, ~~1992). Historical climatology (up to 1980s)based mostly on the western Adriatic data (Artegiani et al., 1997) gives the range for mean surface salinity between 35.4 during summer and 37.3 during winter, while the deep values range between 38.0~~ 3.7 and ~~38.2 (at 30 m). Still, this climatology was encompassing the whole northern Adriatic shelf, from the middle Adriatic depressions, and is not comparable to the climatology off the city of Rovinj.However, these values have changed rapidly in the last decade or so, including rapid oligotrophication observed in the last two decades (Vlašiček et al., 2025). There are several reasons for that : (i) Adriatic-wide changes that affect also the northern Adriatic over yearly scales (Vilibić et al., 2020), and (ii) reduced freshwater load, in particular during some years such as 2022 (Bonaldo et al. , 2023; Aragão et al, 2024).~~

~~Figure 2. As in Fig. 1, but for the northern Adriatic (also referred as the Mediterranean region DJ1 by Manca et al., 2004).~~

~~When examining the available in situ temperature and salinity data in the northern Adriatic in the 20th and 21st centuries (Fig. 2; data sources are the same as in Fig.~~3.7, so the upper-layer temperature deficit is robust and if anything understated. The deficit is also consistent with the large climatological differences of Fig. 1~~), an overall warming trend is apparent despite the large variability expected over wide shelves and rapidly changing regions. As observed in~~ : the Mediterranean median itself warms at 0.41 °C per decade in the surface layer, so a southern Adriatic surface rate of 0.22 °C per decade is a below-median rate even though the difference it accumulates between 1950–1999 and 2000–2025 is large. Ranked against all 28 sub-basins on this pipeline, the southern Adriatic is the sixth slowest-warming at 5–50 m, placing it in the bottom quartile; the northern Adriatic, ~~warming in the northern Adriatic is most pronounced in the subsurface layers (10–30 m), where—particularly during summer—21st century temperatures exceed 20th century values by up to 3 °C. In deeper layers, where waters are primarily~~

advected from the southeast, the temperature increase reaches up to 1 ^circC, similar to the subsurface warming observed in the southern Adriaticby contrast, is the fifth fastest. The upper Adriatic is therefore not uniformly slow either – the deficit is specific to the southern basin.

It should be noted that the sampling distributions vary somewhat between the two centuries, which may introduce biases into the thermohaline climatologies. In particular, 20th-century samples are more concentrated along the western coastline, where freshwater discharges, especially from the Po River, occur (Artegiani et al. Salinity behaves differently from temperature. The salinity ratio is 4.3 at 5–50 m, 1.3 at 75–200 m, 1.9 at 250–600 m and 3.8 at 700–1200 m, so haline amplification is present through the whole column, with a minimum at intermediate depths. Only the thermal amplification is deep-specific: the southern Adriatic is salinifying faster than the Mediterranean median everywhere, but warming faster than it only below 200 m. These ratios are window-mean rates, 1997). However, such biases are likely to primarily affect salinity, which is generally higher along the eastern coastline (Vilibić et al., 2019). what the climatological difference in Figs. 1–2 measures, and are not the acceleration of those rates. Terzić and Vilibić (2026c), on the same dataset, find Mediterranean warming and salinification to be accelerating rather than linear, with the acceleration peaking in the Adriatic–Ionian sector; a quadratic fit to the series used here reproduces that, giving the southern Adriatic $+0.29$ per decade^2 in surface salinity. A basin whose rate was modest early in the window and high late in it has an unremarkable window-mean rate but a large acceleration, so the two statements are compatible.

Despite these potential biases, salinity exhibits an increasing tendency in the surface layers, reducing the seasonal differences between summer, when Po River waters spread across the open northern Adriatic , and winter, when these waters are largely confined to the western coastline. Surface salinity increase is most pronounced during summer, which might be reflect—in addition to the changes in freshwater load and dynamics (Montanari et al., 2023)—the increased evaporation in the 21st century (Skliris et al. , 2018; Kraus et al. , 2019). Apart from summer surface increase, the salinity changes appear to be moderated by enhanced baroclinicity of the water column, which tends to redistribute freshwater more toward the open northern Adriatic and retain it there—thereby decreasing salinity—rather than transporting it along the coastline toward the middle and southern Adriatic (Vilibić et al., 2019). Thermosteric expansion exceeds halosteric contraction, resulting in a general decrease in water density. However, the recent decline in sea level in the northern Adriatic has been attributed to a deficit in the regional water budget, a trend projected to persist in the future (Verri et al., 2024), while steric effects are likely of limited importance in such shallow regions. The deep-layer ratios are the robust part of this comparison; the shallow ones should be read together with the sampling caveats above.

3.4 The intermediate salinity maximum has lost its dominant band

Surface saline lakes (SSLs), a term coined by Terzić et al. (2025b) , resemble near-surface stratifications (e.g., down to ~200 m) in which surface-layer salinity strongly exceeds the salinity below a very sharp negative halocline. The positive density stratification is maintained by strong heat accumulation in the surface layer, such that temperatures in the upper layer are significantly higher than below the strong thermocline, which typically coincides with the negative halocline. The thermocline, halocline and pycnocline are spanning over thin vertical section, typically a few metres wide, The classical

description of the southern Adriatic intermediate layer is of a single salinity maximum, associated with the inflow of Levantine Intermediate Water and typically found between 200 and ~~all occurring at the same depths with rates of changes that may exceed (for extreme manifestations) -0.5 oC m-1, -0.05 m-1 and 0.2 kg m-3 m-1, respectively (Terzić et al. , 2025b). SSLs are generated during springtime heating under conditions of weak wind-driven mixing, when enhanced solar heating is followed by increased evaporation and the separation of the surface (10–20~~ 400 m (Artegiani et al., 1997). We test that description directly by detecting every prominent salinity maximum in each cast rather than one core depth (Sect. 2.7), and asking where those maxima sit.

The change is in where the maxima lie rather than in how many there are. Two maxima are not a modern feature: among casts deep enough to resolve both, 65.8 % carried two in 1950–1999 and 68.6 % in 2000–2025. This is the one quantity in this section that depends on the detection settings: across the grid of Appendix A it rises significantly in some configurations and falls significantly in others, so we draw no conclusion from it beyond the absence of a consistent trend. What did change is their concentration. In 1950–1999 the detections cluster in one band: 28 % of them fall in a single 50 m interval at 100–150 m and 42 % within 100–200 m. This band is where the detections themselves concentrate and is not a definition of the core; it spans the shallower member and the top of the classical 200–400 m range. In 2000–2025 that same band holds only 16 %, and the detections spread through the column in both directions – 43 % now lie above 100 m against 26 % before, and 30 % below 300 m against 17 % (Fig. 4). The historical profile therefore had a dominant intermediate maximum, which a single-core description represents adequately; the modern one does not.

The two features have also moved apart. Measured within each cast, the median separation between them grew from 92 m in 1950–1999 to 113 m in 2000–2025 ($p = 6 \times 10^{-7}$, Mann–Whitney), and the spread of separations grew far more, from an interquartile range of 31–160 m to one of 29–378 m: some casts now carry two maxima very close together and others two that are hundreds of metres apart. Pooled across casts, the deeper member sits at a median 325 m (95 % confidence interval 295–345 m) ~~layer from the underlying water column. During summer and early autumn, these features may intensify as heat accumulation and water losses increase, while they are typically deepened and eventually destroyed during autumn or early winter. The destruction is preconditioned by a weakening of pycnocline intensity at SSL's basement due to salinity increase and temperature decrease in autumn, allowing from wind-driven mixing to break the stratification during first intense storms hitting a region.SSLs are expected to occur mostly occurring at the open ocean, while freshwater discharges may prevent their occurrence in coastal regions, or regions affected by freshwater load (which may nullify the salinity increase near the surface). In a way, SSLs are a phenomenon opposing to barrier layers observed in the tropical oceans (Sprintall and Tomczak, 1992), in which surface freshening on top of thermally-driven pycnocline is increasing the stratification.~~ against 201 m (183–228 m) before, and the shallower at 78 m (75–81 m) against 100 m (86–111 m); the intervals do not overlap for either member. These pooled medians describe the two populations and are not the separation within a cast, which is why they do not subtract to it. Their densities diverged with their depths: the shallower maximum became 0.12 kg m^{-3} lighter as it salinified, while the deeper one changed by only 0.03 kg m^{-3} and so stayed close to its isopycnal. A feature that is simultaneously saltier and markedly lighter cannot be the same water displaced upward, so the two are not one migrating core.

SSLs are frequently observed in the Levantine Basin (Kassis and Korres, 2020)and appear to be common in other Mediterranean basins as well, including the Adriatic Sea (Terzić et al., 2025b). In the era of climate change, characterized by enhanced evaporation, reduced precipitation, and decreased river discharge across most of the Mediterranean (Skliris et al. , 2018; Soto-Navarro et al., 2020; Mamoutos et al. , 2022; Liu et al. , 2025), They have not, however, become sharper. The salinity drop from the weaker maximum to the minimum between the two, which measures how distinctly the pair stands apart, is unchanged: a median of 0.021 in both periods, with overlapping confidence intervals (0.017–0.032 and 0.020–0.023). The maxima are therefore differently placed rather than better resolved.

Two checks support this. Repeating the detection on modern profiles degraded to historical standard depths gives 44.0 % of detections in the 100–200 m band for 1950–1999 against 15.0 % for 2000–2025, against 41.7 % and 15.5 % at native resolution, so the contrast is not an effect of the finer modern sampling. The concentration in that band is higher in 1950–1999 than in 2000–2025 under every combination of the detection parameters we tested, as is the frequency of occurrence of SSLs appears to be increasing compared to the 20th century. However, this increase may include biases due to major shifts in observational capabilities (e.g., Argo profiling floats versus shipborne and moored measurements; Tintoré et al., 2019). excess lightening of the shallow member over the deep one (Fig. A3).

Surface saline lakes may play a crucial role in maintaining downward salt fluxes from the surface to deeper layers, thereby modifying the properties of Levantine Intermediate Water (LIW) and Cretan Intermediate Water (CIW) and contributing to the overall salinization of the Mediterranean Sea (Fedele et al.

3.5 Surface saline lakes: an abrupt shift

Detection rates differ by a factor of 25 between platforms in the Fig. 3 cast set: 0.58 % for SeaDataNet, 3.75 % for the IOR database, 12.14 % for MSFD CTD and 14.87 % for Argo. In 2017 alone, SeaDataNet found one SSL in 37 southern Adriatic casts while Argo found 89 in 191, in the same basin and year. The degradation experiment identifies the cause (Fig. A1): re-sampling Argo profiles onto coarser grids reduces detections from 438 at native 1–5 m spacing to 434 at 2 m, 244 at 5 m, 52 at 10 m and zero on the standard bottle grid (0, 10, 2022). In the Adriatic Sea, such conditions have historically been detected during dry and hot years , associated with reduced river discharge, enhanced evaporation, and strong inflow of saline waters from the Ionian Sea, i.e., during cyclonic BiOS regimes (Mihanović et al.20, 2021).

Figure 3. Percentage of surface saline lakes (SSLs, as defined by Terzić et al. 30, 2025b) occurrence in the upper ocean layer in the southern Adriatic detected on available shipborne CTD and Argo profiling float data between 1985 and 2025: yearly percentage in all casts (top left), separately for 20th and 21st century and seasons (numbers denote number of SSLs per number of casts, top middle), and 21st vs. 20th century seasonal box plots for SSL's density gradient (DG, top right)50, depth (zSG, bottom left) , salinity gradient (SG, bottom middle)and temperature gradient (TG, bottom right). 75, 100 m). At bottle resolution the criterion detects nothing, even in profiles that demonstrably contain a surface saline lake, because it requires a salinity gradient steeper than $-0.01\,\mathrm{m}^{-1}$ across a feature a few metres thick. The near-zero historical occurrence is therefore partly instrumental, and Fig. 3 is built on resolution-matched casts.

~~Following the methodology introduced by Terzić et al.(2025b), and using all available~~ The gate retains 5244 of the 7202 casts for which vertical resolution could be computed. Enough historical data meets it: SeaDataNet holds substantial high-resolution ~~vertical temperature and salinity data from the southern Adriatic (CTD data obtained from the SeaDataNet Pan-European Infrastructure, local Adriatic databases, and Argo data collected by Euro-ARGO ERIC) ,~~ CTD in the southern Adriatic, with a median level spacing of 1 m, so 75 of the 171 casts in 1985–1989 and 1188 of the ~~number of SSLs appears to have been relatively low during the 20th century, with a maximum yearly percentage occurrence of up to 10% (Fig. 3). Such a low percentage also persisted at the beginning of~~ 1543 casts in 1990–1999 satisfy the spacing and level-count criteria, against 2269 of 2270 in 2016–2025 (Table 1). SeaDataNet ends in 2019, so the recent decade rests on Argo and on the Croatian monitoring CTD. On the matched annual series (27 years with at least 20 casts each), the ~~21st century, until 2017, after which the percentage began to exhibit strong interannual variability, ranging between 5%~~ Pettitt test places a level shift after 2014 ($p = 0.029$; Sect. 2.5). Occurrence averages 4.4 % of casts per year before the break and 17.1 % after, a factor of 3.9. The break year does not depend on how the matched set is assembled: restricting it to SeaDataNet and Argo alone, or adding the two Adriatic regional datasets, moves the means only between 4.4 and 4.8 % before and 17.1 and 17.2 % after, and ~~30–40%. This variability is presumably associated with pronounced interannual differences in late-spring to early-autumn surface forcing (surface heating, precipitation and river discharge,~~ leaves the break after 2014 and significant in every case.

The change is seasonal (Fig. 3B). Between 1950–1999 and ~~wind-induced vertical mixing). As previously documented,~~ 2000–2025, summer occurrence rises from 1.1 % (2 of 176 matched casts) to 30.8 % (297 of 965), and autumn from 4.0 % to 12.5 %, whereas winter occurrence stays at or below 1.3 % in both periods, indicating that winter mixing did not weaken comparably.

The properties of the detected cores changed alongside their frequency (Fig. 3C–F): the median core sits shallower than it did (19 m against 33 m), above a much stronger temperature inversion (median -0.64 against $-0.17\,^{\circ}\mathrm{C\,m^{-1}}$) and density step, while the salinity gradient that defines the feature is unchanged, so the modern events are shallower and more sharply capped rather than merely more frequent.

Two qualifications follow. The increase is roughly fourfold rather than the order of magnitude the raw series implies, because resolution matching raises the pre-2014 occurrence rate, against which the increase is measured, from about 1.5 % to about 4.4 %. The shift also cannot be pinned to 2017~~stands out as the onset year of strong Adriatic SSLs (Mihanović et al. , 2021), after which SSLs began occurring much more frequently. Seasonally, the increase in SSL occurrence is most prominent during summer (July–September), by roughly an order of magnitude, while increases are also observed in autumn (October–December) and, to a lesser extent, in spring (April–June). A minimal SSL percentage persists during winter in both centuries, and the absence of any detectable increase likely indicates that vertical mixing during winters did not weaken between the two periods. Salinity gradients gradually develop from spring towards autumn, indicating that evaporation is constantly taking the water from the upper oceanlayer. The temperature,~~ : it falls after 2014, so the defensible statement is that occurrence stepped up during the 2010s, with 2017 the most extreme year within an already elevated regime.

Resolution alone, however, ~~show typical seasonality driven by heat fluxes: weak SSL temperature gradients (TG) in spring, during the formation of SSLs,~~ does not explain the historical rarity. The 1188 casts from the 1990s that do meet the resolution

criteria yield only 2.0 % detections, against 17.6 % in 2016–2025 on a comparable sample. The degradation experiment establishes only that the coarser part of the historical archive could not have detected these features at all, so absence from that part of the record is not evidence of absence from the ocean; the resolution-matched series remains the one that can size the increase, and it shows a threefold to fourfold rise.

3.6 Steric decomposition: the net contribution is negative

Thermosteric and halosteric height are decomposed separately from the Argo record, over 2014–2024, the most recent full decade with continuous float coverage. Over 0–1000 m (Table 3) the thermosteric trend is $+9.80 \pm 2.71$, the halosteric -15.21 ± 2.33 and the net -5.41 ± 2.49 mm yr^{-1} (Fig. A2): halosteric contraction dominates, and the steric term acts to lower local sea level rather than to raise it. On windows reaching back into the sparsely sampled early Argo years (2010 or 2012 to 2025) the net is also negative in the central estimate, at -1.4 to -2.6 mm yr^{-1}, but no longer distinguishable from zero. What holds on every window tested is the structure of the decomposition – thermosteric expansion significantly positive, halosteric contraction significantly negative and larger in magnitude – while the significantly negative net is a property of the well-sampled 2014–2024 decade.

Integration depth explains most of the apparent disagreement with published Mediterranean values. Recomputed on the 0–400 m layer used by Mohamed and Skliris (2022), the thermosteric rate is $+2.26 \pm 1.37$ mm yr^{-1} against their eastern Mediterranean mean of $+2.13 \pm 0.41$: the rates agree once the layers match, and ~~in autumn, during the deterioration of SSLs, while being the strongest during summer. Such gradients are similar to average thermocline seasonality in the Adriatic (Buljan and Zore-Armanda~~three quarters of the southern Adriatic thermosteric signal lies below 400 m. The halosteric term does not converge (-6.81 ± 2.55 against -0.75 ± 0.19), ~~1976; Artegiani et al., 1997) , which—together with seasonality of SSL salinity gradients—indicate that SSL deterioration is preconditioned by temperature decrease and salinity increase in autumn, resulting in weakening of SSL's pycnocline and allowing for wind-induced vertical mixing to break up the stratification of SSLs in full.~~ and that difference is real rather than methodological – Adriatic salinification over 2014–2024 far exceeds the eastern Mediterranean mean over 1993–2019. In the 600–1000 m layer the thermosteric and halosteric trends are individually well determined, $+5.7 \pm 0.9$ and -5.6 ± 1.0 mm yr^{-1}, and compensate almost exactly, leaving a net of $+0.1 \pm 0.5$ mm yr^{-1} that is consistent with zero. The compensation, not the residual, is the result, and it independently confirms the deep density result of Sect. 3.1.

~~When comparing 21st vs 20th century box plots in Fig. 3,~~ These are decadal rates from a single platform over a window that spans the post-2017 episode, and they are not secular climate trends. To place them against a longer baseline, the same quantities are differenced between the two multiplatform climatologies of Sect. 2.2, 1950–1999 and 2000–2025. Converting that difference to a rate requires the time actually separating the two sets of casts. Their nominal midpoints are fifty years apart, but the casts are not evenly spread within either period: the 20th-century ones cluster in the 1990s, so the mean year of the casts entering each climatology is 1993 and 2013 and the effective separation is 19.8 years, not 50. On that baseline the thermosteric difference is $+7.6$ and the halosteric -6.8 mm yr^{-1}, with a net of $+0.8$ mm yr^{-1} that is not distinguishable from zero and that changes sign with platform selection. Set against it, the recent decade differs from it in the ~~structure of~~

SSLs changed slightly between the two centuries. The depth halosteric term alone: the $-15.2\,\mathrm{mm\,yr^{-1}}$ of 2014–2024 is about 2.2 times the $-6.8\,\mathrm{mm\,yr^{-1}}$ of the long baseline, and between 2.0 and 2.6 times it whichever season of the climatology the comparison is made against. The thermosteric terms differ far less, $+9.8$ against $+7.6\,\mathrm{mm\,yr^{-1}}$, a ratio of 1.3. Nearly all of what distinguishes the recent decade is therefore in the salt.

3.7 Salt fingering: the change is below the LIW core

Sorted by depth, the SSL (zSG) decreased by 15–25% in summer and autumn, suggesting that SSLs became shallower, thereby retaining heat and salt closer to the surface. Salinity gradients (SGs)show a general strengthening during summer but weakening during autumn and spring, while the associated temperature gradients (TGs) exhibit the opposite behaviour. This pattern suggests a predominance of temperature effects during the SSL formation phase in spring, after which salinity plays a greater role in maintaining the SSL structure during summer, while decreasing the stratification intensity during autumn (as SSL's temperature are decreasing in that part of a year).Temperature again appears more influential during the SSL decay phase in autumn, implying that warmer autumn conditions may prolong stronger ocean stratification. Finally, density gradients (DGs) show a decrease during summer, which may be linked to weaker summertime winds and reduced precipitation and basin-wide river discharge in 21st century. which have already been documented in both present conditions as well as projected future climates (Soto-Navarro et al., 2020; Bonaldo et al., 2023; Montanari et al. , 2023; da Costa et al. , 2024; Tojčić et al., 2024double-diffusive diagnostics separate cleanly at the base of the classical LIW core (Table 5, Fig. 6).

Dense water generation in the northern Adriatic and the cascading of North Adriatic Dense Water (NAddW) have been recognized for decades as key processes maintaining ventilation and oxygenation of most near-bottom Adriatic waters (Zore-Armanda, 1963; Buljan and Zore-Armanda, 1976; Vilibić et al. , 2023). Dense waters are generated in two main regions of the northern Adriatic: (i) the shallow northern Adriatic shelf (Vested et al., 1998; Beg Paklar et al. , 2001; Kuzmić et al., 2007; Benetazzo et al. , 2014), where severe bora events cool shallow waters to temperatures as low as 4 °C (Vatova, 1934; Mihanović et al., 2013; Raicich et al. , 2013Within the core itself, over 200–400 m, nothing changes that we can distinguish from sampling variability: the finger-favourable fraction is 55.3 % before 2017 and 60.1 % after ($p = 0.07$), and the vigorous fraction – levels with $R_\rho < 2$, at which fingers transport appreciably – is 34.6 % against 33.1 % ($p = 0.37$), occasionally producing potential density anomalies (PDAs) close to or exceeding 30 kg m-3; and (ii)a deeper (up to ~100 m) coastal region of the northeastern Adriatic, recently identified as a secondary dense water formation site, where bora-induced cooling is particularly intense (Grisogono and Belušić, 2009; Janeković et al. , 2014; Mihanović et al. , 2018). Due to strong thermal forcing, these waters reach high densities, spread along the bottom as density currents (Nof, 1983) , and cascade into the Adriatic depressions, namely the Jabuka Pit and the South Adriatic Pit (Artegiani and Salusti, 1987; Marini et al., 2006; Langone et al. , 2016; Pranić et al., 2024). At the bottoms of the Jabuka and South Adriatic pits, a characteristic pattern emerges, consisting of rapid dense-water cascading (lasting several months) followed by slower restoration phases (from years to decades) governed by double-diffusive and other mixing processes (Amorim et al., 2024). This behaviour is commonly referred to as the saw-tooth pattern (Querin et al., 2016; Mihanović et al., 2018). if anything slightly lower. Only stratification weakens, median N^2 falling by 26 %.

~~Until about a decade ago, the saw-tooth pattern was primarily thermally driven, as density variability in the Adriatic depressions was dominated by cooling in the northern Adriatic, resulting in cascading waters of higher density due mainly to lower temperatures (Fig. 4 upper plot; the scheme is based on Querin et al., 2016). However, this regime has changed over the past decade due to salinization of NAddW formation sites in the northern Adriatic (see previous chapters). Concurrently, since 2012, winters and associated bora events have not reached historical levels of severity or duration, including reduced rates of heat loss from~~ Below the core the picture changes. Over 400–600 m the finger-favourable fraction rises from 56.6 % to 63.0 % ($p = 0.001$) and the ~~sea (Terzić et al., 2025a). A decline in bora wind intensity and frequency—combined with reduced freshwater discharge and enhanced evaporation—has been projected by numerous climate studies, including regional ensemble simulations (Bonaldo et al.,~~ vigorous fraction from 28.0 % to 41.2 % ($p = 2 \times 10^{-11}$), while median N^2 falls by 60 %, from 2.50×10^{-6} to 0.99×10^{-6} s^{-2}. In the deep layer, 600–1000 m, the regime was already close to saturation in extent before 2017, occupying 92.1 % of levels, and does not expand further (88.7 % after); what changes there is vigour, and it changes more than anywhere else, from 10.7 % to 38.7 % ($p = 2 \times 10^{-77}$). The deep layer was thus always finger-favourable but only became finger-effective after 2017~~; Belušić Vozila et al., 2019; Moulin et al., 2024) and kilometre-scale climate models (Denamiel et al., 2020). As a result, the dense waters formed~~ : the conditions allowed fingering throughout, and only recently has a large part of the layer reached the density ratios at which fingers actually transport salt.

This depth structure matches the one in Sect. 3.4. The deeper salinity maximum descended from a median 201 to 325 m, that is from the middle of the classical core toward its base, and the share of deeper maxima lying below 400 m rose from 16.1 % to 41.9 % over the same period. The layers in which fingering intensified are the layers the salt has moved into, and the core it has moved out of is the layer in which nothing changed.

Stratification is what drives this rather than any change in the temperature–salinity contrast: N^2 falls significantly in all three layers, and most sharply in the 400–600 m layer where the vigour increase is largest.

The intensification is progressive rather than a step at 2017. In the deep layer the median vigorous fraction per profile is 17 % in 2017 ~~, 2018,~~ itself, close to the earlier level, rises through 2019 (24 %) to a maximum in 2021–2023 (51–61 %) and relaxes to about 30 % in 2025; the 400–600 m layer follows the same course about three years earlier, peaking in 2020. It therefore reaches the layer below the core before it reaches the deep layer, which is the order a downward transfer of salt requires.

4 Discussion

4.1 A coupled advective and local mechanism

The results are consistent with remote and local mechanisms acting together, and with neither alone. Progressively warmer and saltier Eastern Mediterranean source water supplies an increasingly saline reservoir at the southern boundary (Skliris et al., 2025; Schroeder , while local preconditioning determines how and where that salt is redistributed within the basin: reduced river discharge lowers the Adriatic freshwater budget (Verri et al., 2024), and ~~2022 were predominantly haline-driven, produced by relatively weak wintertime cooling of highly saline waters in~~ the ~~dense water formation regions (Terzić et al., 2025a). These haline-driven dense waters were observed to cascade into the Adriatic depressions, reaching even the ~1200 m deep South Adriatic Pit, where~~

newly formed waters exhibit higher salinity and substantially higher temperatures than the resident deep waters (Le Meur et al. , 2025; Martellucci et al. , 2025a).This shift has resulted in an inversion of the traditional saw-tooth pattern, which now departs markedly from its classical form (Fig. 4 bottom plot; the scheme is based on Terzić et al. , 2025a). exceptional salinities of 2017 and their basin-scale preconditioning are documented by Mihanović et al. (2021). We have no observational budget for evaporation or winter mixing. The seasonal breakdown of Sect. 3.5 places the preconditioning in the warm season, since summer and autumn surface-lake occurrence rose sharply while winter occurrence did not, so the change acts on the summer surface layer rather than on winter convection.

Figure 4. Saw-tooth modulation over time at the bottom of the Southern Adriatic Pit, showing dense water cascading and intermittent periods of salt-fingering double diffusion, before early 2010s (up, for PDA adopted from Querin et al. , 2016) and in the warming and saltening climate as observed in the last decade (bottom)The salinity-maximum result constrains the mechanism further. The deeper maximum stayed near its isopycnal, which is what advection of a denser saline core into a warming basin would produce, while the shallower one became much lighter as it salinified, which requires a different and shallower source. These are two pathways rather than one migrating feature, and a single-core description cannot represent both. Mihanović et al. (2021) see the same split in the 2015–2017 episode, with new high-salinity water arriving nearer the surface from 2015 while the saline core deepened, though their excursion is far larger because they track individual floats through a particular sequence of years where we take a climatological median over multi-decadal periods.

Reported LIW depths vary too much between regions to serve as a baseline for any of this. The intermediate salinity maximum lies at 200–500 m for the Mediterranean as a whole and at 300–800 m in the western basin (Schroeder and Chiggiato, 2022) , while Argo places it at 200–600 m Mediterranean-wide (Kubin et al., 2019) and at about 100–250 m in the eastern Mediterranean over 2015–2017 (Fach et al., 2021). The 200–400 m of the classical southern Adriatic description (Artegiani et al., 1997), the range we test against and the one our layers follow, sits within that spread.

The documented changes in temperature and salinity are expected to affect sea level trends in the Adriatic Sea (and beyond), particularly in the deep southern Adriatic. Historically, sea level trends in the Mediterranean have been somewhat lower than global trends, largely due to sterically driven increases in seawater density (Tsimplis and Baker, 2000; Marcos and Tsimplis, 2008). An increase in density was also observed in the deep Adriatic until the early 2000s; however, this trend reversed thereafter (Terzić et al. , 2025a). Recent estimates indicate that thermosteric expansion of the water column amounts to approximately 2.0 cm yr-1, slightly exceeding halosteric contraction estimated at about 1.7 cm yr-1 (Terzić et al., 2025a) . Together with increasing mass input into the Mediterranean Sea (Sannino et al., 2023; Parras-Berrocal et al. , 2025), these processes may resultin a somewhat higher rate of One hypothesis follows, which the present data are consistent with but do not establish: that the depth-dependence of the amplification (Sect. 3.3) is the signature of this same split, with thermal amplification confined to the deep layers because renewal there is episodic while the upper layers are ventilated fast enough by air–sea exchange to track rather than exceed the Mediterranean mean, and haline amplification present through the column because salt arrives both at the surface and at depth. That the same sector emerges as the locus of Mediterranean-wide acceleration (Terzić and Vilibić, 2026c) is consistent with this reading, as is the depth structure of the double-diffusive result.

4.2 Density, sea level and ventilation

The steric decomposition bears directly on the sea level argument. With a net steric contribution of $-5.4 \pm 2.5\,\mathrm{mm\,yr^{-1}}$ the steric term opposes rather than drives local sea level rise~~compared to previous decades, not just in the Adriatic Sea but in the Mediterranean Sea.~~

~~Nevertheless, at least in the northern Adriatic, recent strong salinization and reduced river discharge have resulted in a~~ , so any observed rise in the Southern Adriatic must be mass-driven. This is consistent with Verri et al. (2024), who attribute the recent northern Adriatic sea level decline to a regional water deficit, ~~which has been shown to reduce the rate of sea level rise (Verri et al., 2024). Whether this trend will persist in the future, as projected by climate simulations (Zanchettin et al. , 2021), remains uncertain, as even decadal-scale increases in freshwater discharge may substantially alter present trends (Rubinetti et al., 2022). Under such scenarios, and in combination with the phasing of different contributors to extreme sea levels (e.g., tides, storm surges, seiches; Šepić et al. , 2022), coastal flooding in the Adriatic could increase markedly, particularly in historic cities with valuable cultural heritage (Reimann et al., 2018). Moreover, the increasing frequency of MOSE barrier closures in the Venice Lagoon may have severe ecological consequences (Cibic et al., 2025), not only for the lagoon itself but also for other low-lying Adriatic coastlines (Krvavica and Ružić, 2020; Favaretto et al. , 2025).~~ and with the near-exact deep thermal–haline compensation in Fig. 1. It rests on a single Argo decade: the sign is robust over 2014–2024, but whether it persists cannot be settled from this record.

~~The observed physical changes may have several biogeochemical consequences. First, the increased occurrence of surface saline lakes may strongly reduce vertical fluxes of dissolved oxygen, nutrients, and carbon between surface and subsurface or intermediate layers (Jacox and Edwards, 2011; Breitburg et al.~~Deep ventilation of the pit is episodic. From moorings over 2012–2022, Le Meur et al. (2025) identify gravity currents reaching the deep Southern Adriatic in only four years, 2012, 2017, ~~2018; Bourgeois et al. ,~~ 2018 and 2022~~). Such reductions may substantially alter primary production and microbial food webs (Beg Paklar et al., 2020) and decrease the ocean's capacity for carbon uptake (Cantoni et al., 2024; Martellucci et al., 2025b). Furthermore, changes in the characteristics of North Adriatic Dense Water (NAddW) and its cascading into deep layers may affect oxygen, sediment, and carbon fluxes, as these processes are closely linked to dense water formation events (Ingrosso et al., 2017; Paladini de Mendoza, 2023). For instance, warmer dense waters may transport less oxygen to deep ecosystems, including those in major Adriatic nursery areas such as the Jabuka Pit depressions (Chiarini et al. ~~2022a,b). In addition, a stronger haline contribution relative to thermal forcing in dense water formation may alter the intensity and frequency of cascading events. Reduced cooling requirements for dense water formation could locally enhance deep-layer ventilation, contrary to projections from regional climate models that suggest an overall decline in dense water formation and a shallowing of the Adriatic thermohaline circulation (Parras-Berrocal et al., 2023).~~ ; the first followed an exceptionally strong and prolonged bora outbreak that formed very cold, dense water (Mihanović et al., 2013). Deep properties therefore respond as a series of steps rather than as a gradual drift, each event resetting them before they relax again (Fig. 5), and the sign of the reset has changed: in the earlier regime (Querin et al., 2016) cascading water arrived cold and cooled the deep layer, whereas since 2017 it arrives only weakly cooled but much saltier and leaves the layer warmer and saltier than it found it (Terzić et al., 2025a). The deep trends

of Sect. 3.6 are individually significant, but this saw-tooth is why a decade cannot show whether they are secular. Whether the shift toward haline-driven formation sustains ventilation, because saline water needs less cooling to sink, or degrades it, because the water so formed is warmer and carries less oxygen (Ingrosso et al., 2017; Chiarini et al., 2022), is not resolved by our data.

~~In the shallow northern Adriatic, extreme precipitation events may produce pronounced peaks in freshwater discharge and—as observed in 2024—result in rapid transport of freshened waters over strongly stratified, warm, and saline surface layers. Such events may trigger sudden phytoplankton blooms and mucilage formation when these waters reach the eastern Adriatic coastline (Vilibić et al.~~ The double-diffusive result locates the mechanism. Finger-favourable water grows below the classical LIW core and not within it, which is where the deeper salinity maximum has moved (Sect. 3.7), ~~2025; Neri et al., 2025). Future mucilage events may thus become rarer but more intense, occurring mainly during extreme springtime precipitation episodes, with strong impacts on tourism, fisheries and human health along the Adriatic coast (Rinaldi et al., 1995; Funari and Ade, 1999; Giani et al., 2005, 2012). Overall, increasing stratification in the northern Adriatic may reduce vertical fluxes of oxygen, carbon and nutrients, leading to non-linear ecosystem responses (Vichi et al., 2003) and further oligotrophication (Mentaschi et al., 2024)~~because the density gradient there has weakened enough to let fingers reach full amplitude before ambient shear disrupts them. Salt fingering has therefore become more effective in the layer where the salt now arrives, and below it the deep layer, already saturated in extent, tripled the fraction in which fingers actually transport salt. Salt descending out of the core meets a column newly capable of carrying it further down, though we have not measured a flux.

~~In the deep Adriatic, a shoaling of Levantine and Cretan Intermediate Water (LIW/CIW) inflows could bring these waters closer to the euphotic zone. If such shoaling also occurs in the Ionian Sea, nutrient concentrations may decrease, promoting further oligotrophication of the Adriatic. Conversely, if the LIW/CIW core remains deeper in the Ionian prior to entering the Adriatic, these waters may locally enhance primary production in the South Adriatic Pit through nutrient supply. Similar effects of LIW shoaling on primary production have already been documented in the Levantine Basin (Ozer et al., 2022; Reich et al., 2026).~~ Amorim et al. (2024) report the same transition from the EMSO-E2M3A mooring in this pit, finger-favourable conditions rising from 27 % to 72 % of observations across the winter of 2016/17. Their 350–550 m layer straddles the base of the core, where we also find the change; recomputed on it our diagnostics rise from 48.6 to 60.2 % in extent and 29.1 to 38.8 % in vigour (Table 5). Both analyses find a significant increase there, which is as far as the agreement can be taken, since a mooring sampling one position continuously and a float array sampling the pit every few days do not measure the same quantity.

4.3 Biogeochemical and ecological implications

~~Changes in heat and freshwater exchange between the Adriatic Sea and the atmosphere due to ocean warming may induce substantial impacts on surrounding continental regions, particularly in terms of extreme events (Iakunin et al., 2021; Kunkel et al., 2022; Yang et al., 2024). This is especially relevant for phenomena such as snow enhancement over the Apennines during persistent bora events (Davolio et al.,~~ The following are plausible pathways, not effects quantified here, and we limit them to the changes reported above.

A near-surface salinity maximum has two competing effects on vertical exchange and our analysis resolves neither. It increases the density stability of the upper column, which acts to suppress exchange of oxygen, nutrients and carbon with the intermediate layers (Jacox and Edwards, 2011; Breitburg et al., 2018; Bourgeois et al., 2022), with consequences for production, microbial food webs and air–sea carbon exchange (Cantoni et al., 2024; Martellucci et al., 2025b); the record salinities of 2017) and increased precipitation intensity along Adriatic coastlines (Ivatek-Šahdan et al., 2018). Warming of the Adriatic Sea surface is expected to enhance moisture fluxes into the atmosphere, and regional climate projections consistently indicate an increase in extreme precipitation events along surrounding coasts (Fedele et al. , 2024; Ivušić et al., 2024). Changes in precipitation seasonality, including altered snowfall and snowmelt regimes, are projected to modify river discharge patterns and flood frequency (Tramblay et al. , 2022), leading to increased intensity and destructiveness of flash floods (Ojeda et al., 2022). coincided with bacterial abundances several standard deviations from the mean (Beg Paklar et al., 2020), elevated salinity imposing osmotic stress that constrains growth directly. But salinity decreasing with depth beneath the maximum is itself finger-favourable, so the same feature may instead promote downward transport. Our diagnostics begin at 200 m and cannot say which dominates in the surface layer; dedicated observations there are required.

Beyond direct terrestrial impacts, intense precipitation events may strongly affect coastal marine systems by delivering large amounts of nutrients and sediments over a short period, thereby enhancing rapid productivity in an already warming coastal ocean (Gao et al., 2023). These effects are likely to be particularly pronounced on the northern Adriatic and Albanian shelves, as well as in estuaries and river deltas (Wetz and Yoskowitz, 2013)—from the Po River delta to smaller systems such as the Jadro catchment, the Ofanto estuary and the Krka estuary in the Middle Adriatic (Aragão et al. , 2024). Whether the redistribution of the intermediate maxima promotes or suppresses production likewise depends on the upstream history of the inflowing water, on whether its nutrients were drawn down in the euphotic zone before it entered the basin (Ozer et al., 2022; Reich et al., 2026) , which our results do not resolve.

Closely linked to ocean surface warming, increased evaporation relative to precipitation, and declining mean river discharge, a projected rise in the frequency and intensity of surface saline lakes in the Adriatic and Mediterranean may further amplify marine heatwaves, which are already expected to increase substantially (Darmaraki et al. , 2019; Denamiel, 2025). These trends are anticipated to exert strong impacts on marine biogeochemistry and ecosystems (Smith et al. , 2023).

A substantial increase in bottom water temperature and salinity driven by changes in NAddW source properties has the potential to significantly alter Adriaticbenthic ecosystems. Deep-sea ecosystems and marine protected areas are particularly vulnerable to temperature increases (Chimienti et al., 2021; Kružić et al., 2025), with elevated mortality rates already For ecosystems, documented impacts and projected vulnerabilities should be kept apart. Three effects have been observed in the Adriatic: mass mortality linked to warming (Kružić et al., 2016). Overall, these changes may substantially reduce Adriatic benthic biodiversity, in line with trends observed across the Mediterranean Sea (Chatzimentor et al., 2022; Hassoun et al., 2025).

In response to warming, some benthic species are migrating toward northern Adriatic coastlines (Matić-Skoko et al. , 2022; Bellin and Rossi, 2024). However, the availability of suitable cold refugia is limited . For instance, (Kružić et al., 2016), mussel mortality in coastal waters (Capriotti et al., 2025), and redistribution of benthic species toward northern coastlines

(Matić-Skoko et al., 2022; Bellin and Rossi, 2024). Others remain projections: that further redistribution will be constrained by the basin's semi-enclosed geometry and by the limited cold-water refugia of the middle Adriatic depressions ~~serve as nursery areas for many cold-adapted benthic species (Ercegović, 1956–1958; Chiarini et al., 2022a,b), whose survival depends on the regular renewal of bottom waters by NAddW. As these species cannot migrate further north, they face either adaptation to warmer and more saline conditions or local extinction.Some of these species are commercially exploited (Martinelli et al.~~ (Chiarini et al., 2022; Carlot et al., 2025), with consequences for the fisheries that exploit them (Martinelli et al., 2023; Kamberi et al., 2025 . The link to aquaculture runs through the bottom-water warming and salinification documented in Sect. 3.1 rather than through climate change in general (Cetinić, 2024; Haberle et al., 2024).

4.4 Limitations

The climatological comparison rests on a changing observing system, and we have controlled for this where it is testable – by resolution matching for SSL detection, by degradation experiments for the salinity maxima, and by cruise-day clustering for the difference profiles – but not everywhere. Northern Adriatic salinity remains the weakest element, because 20th-century sampling is concentrated on the western side of a basin with a strong east–west salinity gradient. The Argo-based steric and double-diffusive results describe the Southern Adriatic Pit over a single decade, and a decade cannot separate a secular climate trend from the episodic cycle of deep renewal.

The larger gap is that this is an ocean-side analysis throughout: we establish when the changes occurred and how they are distributed in the vertical, ~~2023),~~ but not what forced them. Wintertime turbulent heat flux anomalies over the northern Adriatic formation region do not share a common cooling signature across the recent cascading years – 2018 and ~~their decline may substantially impact Adriatic fisheries under future climate conditions, as already observed in the present climate (Kamberi et al. , 2025).~~

~~The spreading of larvae along the pycnocline may also be influenced by projected increases in stratification and water-column stability, particularly those associated with the strengthening of surface saline lakes. The migration of many organisms is strongly related to stratification intensity (Röpke et al., 1993; Guillam et al., 2020; Barrier et al., 2024; Granata et al., 2024). A more stable and intensified pycnocline may inhibit verticalmigrations, while increasing the potential for horizontal transport.~~ 2022 carry positive anomalies relative to the 1980–2010 baseline, so the density required for cascading in those years cannot have come from heat loss alone (Terzić et al., 2025a). That is consistent with the mechanism proposed above but is not an attribution of it, and the flux estimate is coarse: reanalyses at this resolution underestimate the cooling along the bora jets (Denamiel et al., 2021), where much of the relevant heat loss occurs. Establishing how much of the change reported here follows from bora frequency, evaporation and river discharge requires a dedicated surface-flux and freshwater budget over the formation regions, resolved finely enough to capture the jets. Until that is done, the mechanism of Sect. 4.1 remains a hypothesis rather than an attribution.

~~In addition to benthic organisms, increased mortality of other marine species has been linked to ocean warming in the Adriatic. For example, elevated temperatures in coastal waters, river deltas, and estuaries have triggered mass mortality events in mussels (Capriotti et al. , 2025). Strong freshwater flushing of estuaries during flash floods may further impact aquaculture~~

activities, including mussel farming (Marguš and Teskeredžić, 1986; Cetinić, 2024). Overall, the impacts of climate change on Adriatic fisheries and aquaculture are diverse and complex (e.g., Santojanni et al. , 2006; Dragičević et al., 2017; Cavraro et al., 2023; Haberle et al., 2024; Kamberi et al., 2025). Beyond the physical processes discussed here, many additional factors contribute to these changes and are therefore not addressed in this study.

5 Conclusions

This article documents several tremendous changes in the Adriatic physical properties and dynamics that are documented to occur in the last decade or so: (1) salinization and warming of the Adriatic, in particular of northern Adriatic shallow regions, including changes in the saline inflow characteristics, (2) changes in the NAddW properties, with less pronounced thermal effect in its generation compared to the haline effect, and (3) more frequent occurrence of so-called surface saline lakes, i.e., vertical stratification characterized by negative halocline near the surface that prevent any fluxes through the pronounced pycnocline. There are many other changes in the physical system, either not documented or locally connected with the observed ones, which are not discussed in this article. Impact and consequences to water density, sea level changes, biogeochemistry, and biological, fisheries and aquaculture impacts coming out of these changes are discussed, being just a selection to these connected with the presented changes among a wide impact of climate changes in the region and globally.

Instructively, Three findings are supported by the analyses presented here. First, southern Adriatic warming and salinification between 1950–1999 and 2000–2025 are significant at every depth and season, but the amplification relative to the discussed impacts are not standalone in relation to other climate impacts. Therefore, a proper assessment of climate change impacts would require an assessment of compound effects and nonlinear interactions in the system (Byrne and Przeslawski, 2013), including adaptability of the system (i.e., marine organisms) to the changes (Somero, 2010). Further, the Adriatic Sea is not self-standing in respect with all discussed physical changes and consequent impact, with biogeochemistry, biology, fisheries and aquaculture connected with the rest of the Mediterranean and beyond (Pertesi et al., 2025). We hope that presenting these changes might instruct researchers to become aware of these potentially structural changes in – the ratio of the median within-window trend in the southern Adriatic to the median across the other Mediterranean sub-basins, computed with one pipeline (Sect. 3.3) – is depth-dependent: 6.1-fold for temperature at 700–1200 m and about half the basin median above 200 m, while haline amplification is present through the whole column, reaching 4.3-fold at the surface and 3.8-fold at 700–1200 m. Second, the Adriatic physical properties and to eventually modify their research activities to take theminto account. increase in near-surface salinity maxima is a genuine level shift after 2014, roughly fourfold, and is demonstrable only once vertical resolution is controlled for. The coarser part of the historical archive could not have detected these features at all, yet even among the historical casts that could, occurrence was far rarer: 2.0 % in the 1990s against 17.6 % in 2016–2025, comparing only casts of comparable vertical resolution. Third, the intermediate salinity maximum has lost the dominant band of the classical description: the share of detected maxima within 100–200 m falls from 42 % to 16 % between the periods, while the share of casts carrying two maxima shows no consistent change. Where two coexist they move apart, the deeper one descending

from a median 201 to 325 m while remaining close to its isopycnal and the shallower one rising from 100 to 78 m; only the shallower one becomes markedly lighter as it salinifies, which points to a different and shallower source.

~~Author Contributions~~

Two further results bear on the mechanism. The steric contribution in the Southern Adriatic Pit over 2014–2024 is -5.4 ± 2.5 mm yr^{-1}, negative rather than positive, so local sea level rise must be mass-driven. Moreover, salt fingering has intensified below the classical intermediate core and not within it, in vigour more than in extent, driven by a weakening of stratification measurable in N^2; the layers into which the deeper salinity maximum has descended are therefore also those newly capable of carrying salt further down.

~~Ivica Vilibić: Conceptualization; Methodology; Writing - Original Draft; Writing - Review & Editing; Funding acquisition. Elena Terzić: Formal analysis; Investigation; Data curation; Visualization; Writing - Review & Editing.~~ The consequences for ventilation, biogeochemistry, regional climate feedbacks and ecosystems remain hypotheses. Testing them requires sustained in situ observing at a vertical resolution able to resolve the features described here, and high-resolution coupled physical–biogeochemical modelling able to represent episodic deep renewal. It would also be served by an update of the SeaDataNet Mediterranean aggregation, which currently ends in 2019: the most recent six years of shipborne hydrography are precisely those in which the changes reported here developed, and at present only Argo covers them.

~~Competing interests~~

Code and data availability. The cleaned in situ data are archived by Terzić and Vilibić (2026a) and the analysis code and derived tables by Terzić and Vilibić (2026b). The in situ record ends in 2019; the 2020–2025 part of the 2000–2025 window is supplied by Argo. SeaDataNet Mediterranean aggregated dataset SDC_MED_DATA_TS_V2 is available from https://www.seadatanet.org; Argo data from Euro-Argo ERIC, https://www.euro-argo.eu. Argo floats used are listed in Table 4. Floats 6903805 and 6901865 were excluded from the steric analysis because their profiles do not reach 1000 dbar in the Southern Adriatic Pit; all other ascending profiles reaching 1000 dbar were retained.

~~The authors declare no competing interest.~~

Author contributions. ET: conceptualisation, methodology, formal analysis, investigation, data curation, software, visualisation, writing – original draft, writing – review and editing. IV: conceptualisation, methodology, writing – original draft, writing – review and editing, funding acquisition.

~~Acknowledgements~~

Competing interests. The authors declare that they have no competing interests.

Acknowledgements. We are grateful to all researchers ~~that bring forward concepts and did hard work on the Adriatic climate studies and in collection of the ocean data. In particular, we~~ who developed the concepts and collected the observations on which this study rests. We acknowledge the provision of temperature and salinity data by the SeaDataNet Pan-European Infrastructure, ~~https://www.seadatanet.org, Euro-ARGO ERIC, https://www.euro-argo.eu,~~ Euro-Argo ERIC, the Institute of Oceanography and Fisheries, ~~http://www.izor.hr, the Rudjer Bošković Institute, https://www.irb.hr, and various~~ the Ruđer Bošković Institute, and Italian marine research institutions.

~~Financial support~~

~~This research has been supported by~~ This research was supported by the Croatian Science Foundation through projects GLOMETS (~~Grant IP-2022-10-3064) ,~~ IP-2022-10-3064) and C3PO (~~Grant IP-2022-10-9139~~IP-2022-10-9139) and the incoming mobility scheme for post-doctoral researchers (MOBDOL-2023-12), ~~Interreg Italy-Croatia~~ the Interreg Italy–Croatia Programme 2021–2027 project AdriaClimPlus (~~Grant~~ ITHR0200333)~~and~~ , and the EU NextGeneration project AdriaClimRisk (~~Grant~~ PK.3.4.17.0001).

~~References~~

References

Amorim, F. L. L., Le Meur, J., Wirth, A., and Cardin, V.: Tipping of the double-diffusive regime in the southern Adriatic Pit in 2017 in connection with record high-salinity values, Ocean Sci., 20, 463-474, https://doi.org/10.5194/os-20-463-2024, 2024.

Artegiani, A., Bregant, D., Paschini, E., Pinardi, N., Raicich, F., Russo, A.: The Adriatic Sea general circulation. Part I: Air–sea interactions and water mass structure. J. Phys. Oceanogr., 27, 1492–1514, https://doi.org/10.1175/1520-0485(1997)027<1492:TASGCP>2.0.CO;2, 1997.

Beg Paklar, G., Vilibić, I., Grbec, B., Matić, F., Mihanović, H., Džoić, T., et al.: Record-breaking salinities in the middle Adriatic during summer 2017 and concurrent changes in the microbial food web. Prog. Oceanogr., 185, 102345, https://doi.org/10.1016/j.pocean.2020.102345, 2020.

Bellin, N., Rossi, V.: Modeling the effects of climate change on the habitat suitability of Mediterranean gorgonians. Biodivers. Conserv., 33, 929–948, https://doi.org/10.1007/s10531-024-02779-z, 2024.

Bourgeois, T., Goris, N., Schwinger, J., Tjiputra, J. F.: Stratification constrains future heat and carbon uptake in the Southern Ocean between 30°S and 55°S. Nat. Commun., 13, 340, https://doi.org/10.1038/s41467-022-27979-5, 2022.

Breitburg, D., Levin, L. A., Oschlies, A., Grégoire, M., Chavez, F. P., Conley, D. J.: Declining oxygen in the global ocean and coastal waters. Science, 359, 6371, https://doi.org/10.1126/science.aam7240, 2018.

Bretherton, C. S., Widmann, M., Dymnikov, V. P., Wallace, J. M., and Bladé, I.: The effective number of spatial degrees of freedom of a time-varying field, J. Climate, 12, 1990-2009, https://doi.org/10.1175/1520-0442(1999)012<1990:TENOSD>2.0.CO;2, 1999.

Cantoni, C., De Vittor, C., Faganeli, J., Giani, M., Kovač, N., Malej, A.: Carbonate system and acidification of the Adriatic Sea. Mar. Chem., 267, 104462, https://doi.org/10.1016/j.marchem.2024.104462, 2024.

Capriotti, M., Bracchetti, L., Cocci, P., Mazzocchi, V., Fazzini, M., Corvaro, F., et al.: In situ investigation of ecological and molecular stress mechanisms triggered by marine heat waves in Adriatic populations of the Mediterranean mussel. Diversity, 17, 385, https://doi.org/10.3390/d17060385, 2025.

Carlot, J., Galobart, C., Gómez-Gras, D., Santamaría, J., Golo, R., Siniet, M., et al.: Vulnerability of benthic trait diversity across the Mediterranean Sea following mass mortality events. Nat. Commun., 16, 1571, https://doi.org/10.1038/s41467-025-55949-0, 2025.

Cetinić, A. B.: Shellfisheries in Croatia: from manual collection to contemporary practices, Naše More, 71, 154-165, https://doi.org/10.17818/NM/2024/3.8, 2024.

Chiarini, M., Guicciardi, S., Zacchetti, L., Domenichetti, F., Canduci, G., Angelini, S., et al.: Short-term evaluation of changes in fisheries management measures in the Pomo/Jabuka Pits area. Sustainability, 14, 7742, https://doi.org/10.3390/su14137742, 2022.

Civitarese, G., Gačić, M., Lipizer, M., Borzelli, G. L. E.: On the impact of the BiOS on the Adriatic and Ionian Seas. Biogeosciences, 7, 3987–3997, https://doi.org/10.5194/bg-7-3987-2010, 2010.

Civitarese, G., Gačić, M., Batistić, M., et al.: The BiOS mechanism: History, theory, implications. Prog. Oceanogr., 216, 103056, https://doi.org/10.1016/j.pocean.2023.103056, 2023.

Cushman-Roisin, B. and Korotenko, K. A.: Mesoscale-resolving simulations of summer and winter bora events in the Adriatic Sea, J. Geophys. Res.-Oceans, 112, C11S91, https://doi.org/10.1029/2006JC003516, 2007.

Denamiel, C., Tojčić, I., and Vilibić, I.: Balancing accuracy and efficiency of atmospheric models in the northern Adriatic during severe bora events, J. Geophys. Res.-Atmos., 126, e2020JD033516, https://doi.org/10.1029/2020JD033516, 2021.

Fach, B. A., Orek, H., Yilmaz, E., Tezcan, D., Salihoglu, I., Salihoglu, B., et al.: Water mass variability and Levantine Intermediate Water formation in the Eastern Mediterranean between 2015 and 2017, J. Geophys. Res.-Oceans, 126, e2020JC016472, https://doi.org/10.1029/2020JC016472, 2021.

Gačić, M., Civitarese, G., Miserocchi, S., Cardin, V., Crise, A., and Mauri, E.: The open-ocean convection in the Southern Adriatic: a controlling mechanism of the spring phytoplankton bloom, Cont. Shelf Res., 22, 1897–1908, https://doi.org/10.1016/S0278-4343(02)00050-X, 2002.

Gačić, M., Borzelli, G. L. E., Civitarese, G., Cardin, V., and Yari, S.: Can internal processes sustain reversals of the ocean upper circulation? The Ionian Sea example, Geophys. Res. Lett., 37, L09608, https://doi.org/10.1029/2010GL043216, 2010.

Haberle, I., Hackenberger, D. K., Djerdj, T., Bavčević, L., Geček, S., Hackenberger, B. K., et al.: Effects of climate change on gilthead seabream aquaculture in the Mediterranean, Aquaculture, 578, 740052, https://doi.org/10.1016/j.aquaculture.2023.740052, 2024.

Holt, J., Katavouta, A., Hopkins, J., Amoudry, L. O., Appendini, C. M., Arneborg, L., et al.: Future climate projections in the global coastal ocean, Prog. Oceanogr., 235, 103497, https://doi.org/10.1016/j.pocean.2025.103497, 2025.

Ingrosso, G., Bensi, M., Cardin, V., and Giani, M.: Anthropogenic CO2 in a dense water formation area of the Mediterranean Sea, Deep-Sea Res. Part I, 123, 118–128, https://doi.org/10.1016/j.dsr.2017.04.004, 2017.

IOC, SCOR and IAPSO: The international thermodynamic equation of seawater – 2010: Calculation and use of thermodynamic properties, IOC Manuals and Guides No. 56, UNESCO, Paris, https://doi.org/10.25607/OBP-1662, 2010.

Jacox, M. G. and Edwards, C. A.: Effects of stratification and shelf slope on nutrient supply in coastal upwelling regions, J. Geophys. Res.-Oceans, 116, C03019, https://doi.org/10.1029/2010JC006547, 2011.

Juza, M., Fernández-Mora, À., Tintoré, J.: Sub-regional marine heat waves in the Mediterranean Sea from observations: long-term surface changes, sub-surface and coastal responses, Front. Mar. Sci., 9, 785771, https://doi.org/10.3389/fmars.2022.785771, 2022.

Kamberi, E., Hala, E., and Möllmann, C.: Evidence of climate-driven regime shifts in Adriatic Sea fisheries, Sci. Mar., 89, e108, https://doi.org/10.3989/scimar.05566.108, 2025.

Kružić, P., Rodić, P., Popijač, A., and Sertić, M.: Impacts of temperature anomalies on mortality of benthic organisms in the Adriatic Sea, Mar. Ecol., 37, 1190–1209, https://doi.org/10.1111/maec.12293, 2016.

Kubin, E., Poulain, P.-M., Mauri, E., Menna, M., and Notarstefano, G.: Levantine intermediate and Levantine deep water formation: an Argo float study from 2001 to 2017, Water, 11, 1781, https://doi.org/10.3390/w11091781, 2019.

Kunze, E.: Limits on growing, finite-length salt fingers: a Richardson number constraint, J. Mar. Res., 45, 533–556, https://doi.org/10.1357/002224087788326885, 1987.

Le Meur, J., Wirth, A., de Mendoza, F. P., Miserocchi, S., and Cardin, V.: Intermittent supply of dense water to the deep South Adriatic Pit: an observational study, Front. Mar. Sci., 12, 1516780, https://doi.org/10.3389/fmars.2025.1516780, 2025.

Manca, B. B., Burca, M., Giorgetti, A., Coatanoan, C., Garcia, M. J., and Iona, A.: Physical and biochemical averaged vertical profiles in the Mediterranean regions: an important tool to trace the climatology of water masses and to validate incoming data from operational oceanography, J. Mar. Syst., 48, 83–116, https://doi.org/10.1016/j.jmarsys.2003.11.025, 2004.

Marini, M., Russo, A., Paschini, E., Grilli, F., and Campanelli, A.: Short-term physical and chemical variations in the bottom water of middle Adriatic depressions, Clim. Res., 31, 227–237, https://doi.org/10.3354/cr031227, 2006.

Martellucci, R., Dentico, C., Coppola, L., Skjelvan, I., Giani, M., Pensieri, S., et al.: Air–sea CO2 exchange in the Eastern Atlantic and the Mediterranean Sea based on autonomous surface measurements, Front. Mar. Sci., 12, 1633617, https://doi.org/10.3389/fmars.2025.1633617, 2025b.

Martinelli, M., Zacchetti, L., Belardinelli, A., Domenichetti, F., Scarpini, P., Penna, P., et al.: Changes in abundance and distribution of the sea pen, Funiculina quadrangularis, in the central Adriatic Sea (Mediterranean basin) in response to variations in trawling intensity, Fishes, 8, 347, https://doi.org/10.3390/fishes8070347, 2023.

Matić-Skoko, S., Pavičić, M., Šepić, J., Janeković, I., Vrdoljak, D., Vilibić, I., et al.: Impacts of sea bottom temperature on CPUE of European lobster Homarus gammarus (Linnaeus, 1758; Decapoda, Nephropidae) in the Eastern Adriatic Sea, Front. Mar. Sci., 9, 891197, https://doi.org/10.3389/fmars.2022.891197, 2022.

Maze, G. and Balem, K.: argopy: A Python library for Argo ocean data analysis, J. Open Source Softw., 5, 2425, https://doi.org/10.21105/joss.02425, 2020.

Mihanović, H., Vilibić, I., Carniel, S., Tudor, M., Russo, A., Bergamasco, A., et al.: Exceptional dense water formation on the Adriatic shelf in the winter of 2012, Ocean Sci., 9, 561–572, https://doi.org/10.5194/os-9-561-2013, 2013.

Mihanović, H., Vilibić, I., Šepić, J., Matić, F., Ljubešić, Z., Mauri, E., et al.: Observation, preconditioning and recurrence of exceptionally high salinities in the Adriatic Sea, Front. Mar. Sci., 8, 672210, https://doi.org/10.3389/fmars.2021.672210, 2021.

Mohamed, B. and Skliris, N.: Steric and atmospheric contributions to interannual sea level variability in the eastern Mediterranean Sea over 1993-2019, Oceanologia, 64, 50-62, https://doi.org/10.1016/j.oceano.2021.09.001, 2022.

Ozer, T., Rahav, E., Gertman, I., Sisma-Ventura, G., Silverman, J., and Herut, B.: Relationship between thermohaline and biochemical patterns in the Levantine upper and intermediate water masses, Southeastern Mediterranean Sea (2013–2021), Front. Mar. Sci., 9, 958924, https://doi.org/10.3389/fmars.2022.958924, 2022.

Pettitt, A. N.: A non-parametric approach to the change-point problem, J. Roy. Stat. Soc. C-App., 28, 126-135, https://doi.org/10.2307/2346729, 1979.

Pranić, P., Denamiel, C., Janeković, I., and Vilibić, I.: Multi-model analysis of the Adriatic dense-water dynamics, Ocean Sci., 19, 649–670, https://doi.org/10.5194/os-19-649-2023, 2023.

Querin, S., Bensi, M., Cardin, V., Solidoro, C., Bacer, S., Mariotti, L., Stel, F., and Malaspina, S.: Saw-tooth modulation of the deep-water thermohaline properties in the southern Adriatic Sea, J. Geophys. Res.-Oceans, 121, 4585–4600, https://doi.org/10.1002/2015JC011522, 2016.

Reich, T., Belkin, N., Sisma-Ventura, G., Hauzer, H., Berman-Frank, I., and Rahav, E.: Does oligotrophy favor chemoautotrophy over photoautotrophy?, Prog. Oceanogr., 241, 103633, https://doi.org/10.1016/j.pocean.2025.103633, 2026.

Richardson, C. M., Peucker-Ehrenbrink, B., Wyatt, S., Bourbonnais, A., Hatje, V., Frey, C., et al.: Effects of climate change on river and groundwater nutrient inputs to the coastal ocean, Commun. Earth Environ., 6, 761, https://doi.org/10.1038/s43247-025-02594-6, 2025.

Roether, W., Manca, B. B., Klein, B., Bregant, D., Georgopoulos, D., Beitzel, V., et al.: Recent changes in eastern Mediterranean deep waters, Science, 271, 333–335, https://doi.org/10.1126/science.271.5247.333, 1996.

Schlitzer, R., Roether, W., Oster, H., Junghaus, H.-G., Hausmann, M., Johannsen, H., et al.: Chlorofluoromethane and oxygen in the Eastern Mediterranean, Deep-Sea Res., 38, 1531–1551, https://doi.org/10.1016/0198-0149(91)90088-W, 1991.

Schmitt, R. W.: Double diffusion in oceanography, Annu. Rev. Fluid Mech., 26, 255-285, https://doi.org/10.1146/annurev.fl.26.010194.001351, 1994.

Schroeder, K. and Chiggiato, J. (Eds.): Oceanography of the Mediterranean Sea: An Introductory Guide, Elsevier, Amsterdam, 558 pp., https://doi.org/10.1016/C2020-0-01415-3, 2022.

Schroeder, K., Chiggiato, J., Josey, S. A., Borghini, M., Aracri, S., and Sparnocchia, S.: Rapid response to climate change in a marginal sea, Sci. Rep., 7, 4065, https://doi.org/10.1038/s41598-017-04455-5, 2017.

SeaDataNet: Data quality control procedures, version 2.0, https://www.seadatanet.org/content/download/596/file/SeaDataNet_QC_procedures_V2_(May_2010).pdf, 2010.

Simoncelli, S., Schaap, D., and Schlitzer, R.: Mediterranean Sea – Temperature and salinity Historical Data Collection SeaDataCloud V2 (SDC_MED_DATA_TS_V2) [Dataset], SeaDataNet, https://doi.org/10.12770/2a2aa0c5-4054-4a62-a18b-3835b304fe64, 2020.

Skliris, N., Marsh, R., Breedon, M., and Josey, S. A.: Accelerated warming and salinification of the Mediterranean Sea: Implications for dense water formation, J. Mar. Sci. Eng., 13, 25, https://doi.org/10.3390/jmse13010025, 2025.

Terzić, E., Cardin, V., Le Meur, J., Dunić, N., Vodopivec, M., and Vilibić, I.: Unprecedented warming and salinization observed in the deep Adriatic, Limnol. Oceanogr. Lett., 10, 888–898, https://doi.org/10.1002/lol2.70051, 2025a.

Terzić, E., Gardiol, C., and Vilibić, I.: Surface saline lakes in the Mediterranean Sea, Ocean Sci., 21, 1441–1459, https://doi.org/10.5194/os-21-1441-2025, 2025b.

Terzić, E. and Vilibić, I.: Cleaned Adriatic in situ hydrographic data (1952–2023) for a Mediterranean thermohaline acceleration analysis [Dataset], Zenodo, https://doi.org/10.5281/zenodo.20345373, 2026a.

Terzić, E. and Vilibić, I.: MedClim analysis code for Mediterranean thermohaline acceleration analysis [Software], Zenodo, https://doi.org/10.5281/zenodo.20410481, 2026b.

Terzić, E. and Vilibić, I.: Observational evidence for accelerated warming and salinification propagating into the deep Mediterranean, Geophys. Res. Lett., 53, e2026GL124518, https://doi.org/10.1029/2026GL124518, 2026c.

Tintoré, J., Pinardi, N., Álvarez-Fanjul, E., Aguiar, E., Álvarez-Berastegui, D., Bajo, M., et al.: Challenges for sustained observing and forecasting systems in the Mediterranean Sea, Front. Mar. Sci., 6, 568, https://doi.org/10.3389/fmars.2019.00568, 2019.

Verri, G., Furnari, L., Gunduz, M., Senatore, A., Santos da Costa, V., De Lorenzis, A., et al.: Climate projections of the Adriatic Sea: role of river release, Front. Climate, 6, 1368413, https://doi.org/10.3389/fclim.2024.1368413, 2024.

Vilibić, I., Matijević, S., Šepić, J. and Kušpilić, G.: Changes in the Adriatic oceanographic properties induced by the Eastern Mediterranean Transient, Biogeosci., 9, 2085–2097, https://doi.org/10.5194/bg-9-2085-2012, 2012.

Vilibić, I., Zemunik, P., Šepić, J., Dunić, N., Marzouk, O., Mihanović, H., et al.: Present-climate trends and variability in thermohaline properties of the northern Adriatic shelf, Ocean Sci., 15, 1351–1362, https://doi.org/10.5194/os-15-1351-2019, 2019.

Vilibić, I., Pranić, P. and Denamiel, C.: North Adriatic Dense Water: lessons learned since the pioneering work of Mira Zore-Armanda 60 years ago, Acta Adriat., 64, 53–78, https://doi.org/10.32582/aa.64.1.11, 2023.

Wagawa, T., Igeta, Y. and Abe, S.: Warming and springtime freshening trend in the southeastern Sea of Japan revealed by observational data, Geophys. Res. Lett., 52, e2025GL118631, https://doi.org/10.1029/2025GL118631, 2025.

Wang, G., Cheng, L., Boyer, T., and Li, C.: Halosteric sea level changes during the Argo era, Water, 9, 484, https://doi.org/10.3390/w9070484, 2017.

Wong, A., Keeley, R., and Carval, T., and the Argo Management Team: Argo Quality Control Manual for CTD and Trajectory Data. Version 3.7. https://doi.org/10.13155/33951, 2023.

Zore-Armanda, M.: Les masses d'eau de la mer Adriatique, Acta Adriat., 10, 5–88, 1963.

Table 1. Observational dataset inventory. Counts are retained casts entering the climatologies behind Figs. 1–2. DJ1 and DJ3 are the northern and southern Adriatic polygons defined in the `Basins` package and labelled after the sub-basin nomenclature of Manca et al. (2004); they follow the coastline and bathymetry rather than that paper's boundaries (Sect. 2.2). Bounding boxes are given because the regions are polygons rather than rectangles; their full extent is shown in Figs. 1 and 2. In (b), note the 20th-century summer count in DJ3 (444), the sparsest season–period combination. In (e), the shallowest bin centre of 5 m spans the layer in which the two periods are sampled least alike, and is not interpreted in summer (Sect. 3.1).

(a) Casts by source, region and period

Region	Source	1950–1999	2000–2025	Total
DJ1	SeaDataNet	8903	11014	19917
DJ1	RBI northern Adriatic transect 1979–2018	984	1037	2021
DJ1	IOR Adriatic database 1987–2019	731	829	1560
DJ1	Croatian MSFD / JADMON CTD 2019–2023	0	429	429
DJ1	Argo	0	293	293
DJ3	SeaDataNet	3291	3289	6580
DJ3	Argo	0	2946	2946
DJ3	IOR Adriatic database 1987–2019	141	323	464
DJ3	Croatian MSFD / JADMON CTD 2019–2023	0	96	96

(b) Casts by season

Region	Period	JFM	AMJ	JAS	OND	Total
DJ1	1950–1999	1946	2726	3847	2099	10618
DJ1	2000–2025	3388	2639	4104	3471	13602
DJ3	1950–1999	1028	1163	444	797	3432
DJ3	2000–2025	1227	1721	1852	1854	6654

(c) Casts by maximum depth reached [m]

Region	Period	0–50	50–200	200–600	600–1000	≥1000
DJ1	1950–1999	9931	687	0	0	0
DJ1	2000–2025	12697	905	0	0	0
DJ3	1950–1999	151	1009	804	1076	392
DJ3	2000–2025	1171	900	1005	2618	960

(d) Region boundaries (polygon bounding box)

Region	Name	Longitude	Latitude
DJ1	Northern Adriatic	12.065–15.538 °E	43.623–45.809 °N
DJ3	Southern Adriatic	15.888–20.021 °E	39.790–42.940 °N

(e) Processing parameters

Bin centres (m): 5, 10, 20, 30, 40, 50, 75, 100, 125, 150, 200, 250, 300, 400, 500, 600, 700, 800, 900, 1000, 1100, 1200. Minimum fractional coverage per level: 0.05 (both T and S). Second-pass outlier rejection: 1.0 standard deviation. Accepted quality flags: 1 and 2 (SeaDataNet and Argo). Equation of state: TEOS-10; σ_0 referenced to 0 dbar.

Table 2. Warming and salinification rates for 2000–2025, Adriatic against Mediterranean, from an identical pipeline, binning, quality control and estimator on both sides. Mediterranean values are the median across sub-basins outside the Adriatic, with the interquartile range in brackets; Adriatic values are the median across depth bins within the layer. Trends resting on fewer than 24 months are excluded, which is why DJ1 has no entry below 200 m. DJ1 is reported only to 50 m, because below that the shelf rests on 905 casts against 12 697 above it (Sect. 2.3).

Variable	Layer	N. Adr	S. Adr	Mediterranean	N/Med	S/Med
T [°C decade^{-1}]	5–50 m	+0.600	+0.223	+0.406 (+0.264 to +0.509)	1.5	0.5
T	75–200 m	—	+0.249	+0.342 (+0.266 to +0.400)	—	0.7
T	250–600 m	—	+0.333	+0.222 (+0.166 to +0.291)	—	1.5
T	700–1200 m	—	+0.429	+0.070 (+0.037 to +0.111)	—	**6.1**
S [decade^{-1}]	5–50 m	+0.154	+0.222	+0.051 (−0.032 to +0.097)	3.0	**4.3**
S	75–200 m	—	+0.101	+0.076 (+0.022 to +0.112)	—	1.3
S	250–600 m	—	+0.125	+0.067 (+0.055 to +0.083)	—	1.9
S	700–1200 m	—	+0.122	+0.032 (+0.014 to +0.044)	—	**3.8**

Table 3. Steric sea level trends in the Southern Adriatic Pit, 2014–2024, from deseasoned monthly means of Argo profiles. Intervals are 95 % confidence intervals on the trend, computed with an effective sample size that accounts for residual autocorrelation (Sect. 2.8); they are not standard deviations of the underlying series, and are wide because the effective sample size is a fraction of the number of months. Eastern Mediterranean values are from Mohamed and Skliris (2022) for 1993–2019 and are shown on their own integration layer.

Layer / source	Thermosteric [mm yr^{-1}]	Halosteric [mm yr^{-1}]	Net [mm yr^{-1}]
This study, 0–1000 m	**+9.80 ± 2.71**	**−15.21 ± 2.33**	**−5.41 ± 2.49**
This study, 0–700 m	+5.30 ± 2.19	−11.03 ± 2.54	−5.73 ± 2.28
This study, 0–400 m	+2.26 ± 1.37	−6.81 ± 2.55	−4.55 ± 1.73
This study, 600–1000 m	+5.7 ± 0.9	−5.6 ± 1.0	+0.1 ± 0.5
Eastern Mediterranean, 0–400 m, 1993–2019	+2.13 ± 0.41	−0.75 ± 0.19	—

Table 4. Argo floats contributing to the Southern Adriatic Pit analyses (steric decomposition and subsurface salinity maxima), restricted to ascending profiles reaching at least 1000 dbar.

WMO	Profiles	First	Last	Max. pressure [dbar]
1900848	13	2010-04	2014-04	1184.6
3901978	16	2018-10	2019-09	1220.9
3902626	34	2024-12	2025-09	1227.0
6900979	8	2013-08	2013-11	1173.0
6901040	25	2012-03	2014-05	1216.0
6901822	100	2013-03	2017-12	1227.9
6901827	68	2013-09	2018-05	1207.6
6901862	6	2015-03	2015-04	1018.4
6902848	46	2020-04	2022-11	1223.9
6903178	65	2015-10	2016-08	1222.7
6903197	27	2016-04	2017-02	1016.5
6903236	3	2018-11	2018-11	1213.3
6903250	57	2018-10	2021-01	1020.9
6903781	8	2020-07	2021-01	1228.0
6903799	166	2021-05	2025-09	1230.8
6903821	12	2024-07	2025-01	1151.3
6903825	40	2022-12	2025-08	1017.8

Table 5. Salt-finger diagnostics by layer in the Southern Adriatic Pit, from 694 Argo profiles split before and from 2017 (257 and 437 profiles). Layers are those used throughout the paper: the classical 200–400 m LIW salinity-maximum range (Sect. 3.4), the 400–600 m layer immediately below it, and the deep layer. Extent is the percentage of levels in the salt-finger regime, vigour the percentage with $R_\rho < 2$, and N^2 the median squared buoyancy frequency. Values are means across profiles and p-values are two-sided Mann–Whitney tests on the per-profile layer statistics; those below 0.05 are in bold. Nothing changes significantly inside the core. The last row is the 350–550 m layer instrumented at the EMSO-E2M3A mooring, given only so that our diagnostics can be compared with Amorim et al. (2024) in Sect. 4.2; it straddles the base of the core and is not one of our layers.

	Extent [%]			Vigour [%]			N^2 [10^{-6} s^{-2}]		
Layer	<2017	≥2017	p	<2017	≥2017	p	<2017	≥2017	p
200–400 m *(LIW core)*	55.3	60.1	0.068	34.6	33.1	0.37	1.96	1.44	$\mathbf{7 \times 10^{-9}}$
400–600 m	56.6	63.0	**0.001**	28.0	41.2	$\mathbf{2 \times 10^{-11}}$	2.50	0.99	$\mathbf{4 \times 10^{-43}}$
600–1000 m	92.1	88.7	$\mathbf{8 \times 10^{-24}}$	10.7	38.7	$\mathbf{2 \times 10^{-77}}$	2.55	1.72	$\mathbf{2 \times 10^{-88}}$
350–550 m (mooring layer)	*48.6*	*60.2*	8×10^{-10}	*29.1*	*38.8*	2×10^{-7}	*2.51*	*0.96*	2×10^{-39}

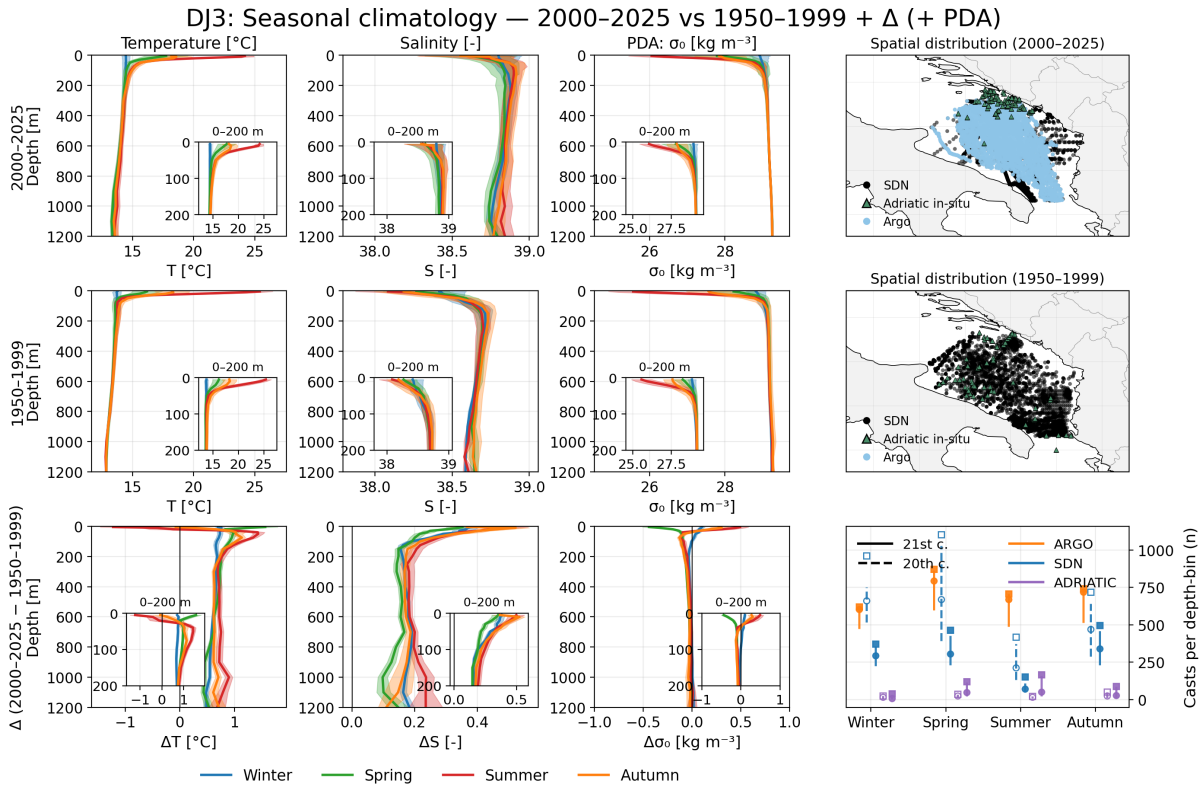


Figure 1. Seasonal climatology of the southern Adriatic (DJ3, Sect. 2.2) from all available in situ sources. Rows: 2000–2025 (top), 1950–1999 (middle), and their difference (bottom); columns: temperature, salinity, potential density anomaly, and observational support. Colours denote seasons. Insets expand the upper 200 m. In the two period rows the shading is ± 1 standard deviation, the spread of the observations contributing to each level. In the difference row it is the 95 % confidence interval on the difference, obtained from a bootstrap over cruise-days so that casts taken within one cruise are not counted as independent (Sect. 2.3); that is the band against which significance should be judged. The right column shows the spatial distribution of casts by source for each period, and the sampling-support panel gives casts per depth bin by platform and season: means as squares, medians as circles, ranges as vertical lines, solid for 2000–2025 and dashed for 1950–1999.

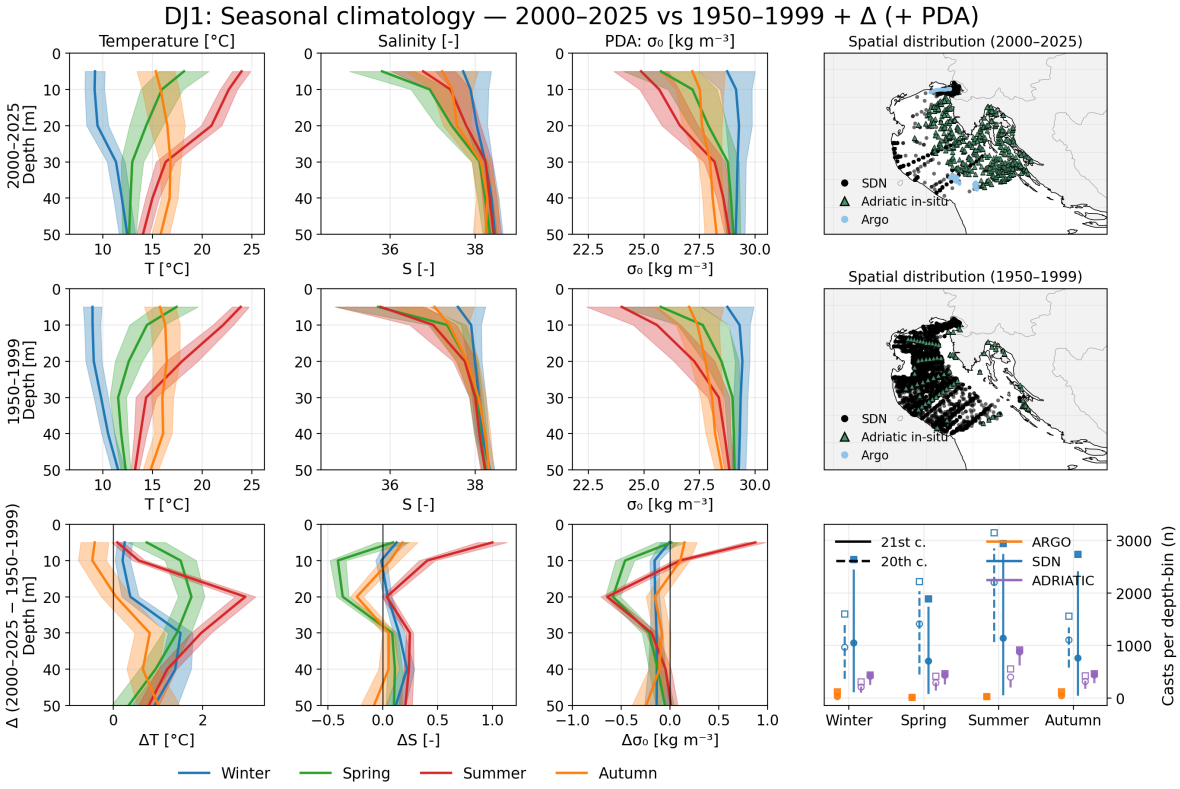


Figure 2. As Fig. 1, but for the northern Adriatic (DJ1, Sect. 2.2) and restricted to 0–50 m. Below 50 m the northern shelf carries fewer than 700 casts per period against more than 12 000 above it (Table 1), and the fitted trend changes sign with the analysis window, so deeper levels are not shown. Confidence intervals are wider relative to the signal than in Fig. 1 because cast clustering within cruises is stronger on the shelf, with variance inflation factors of 5.7–6.3 against 1.8–2.2 in the south.

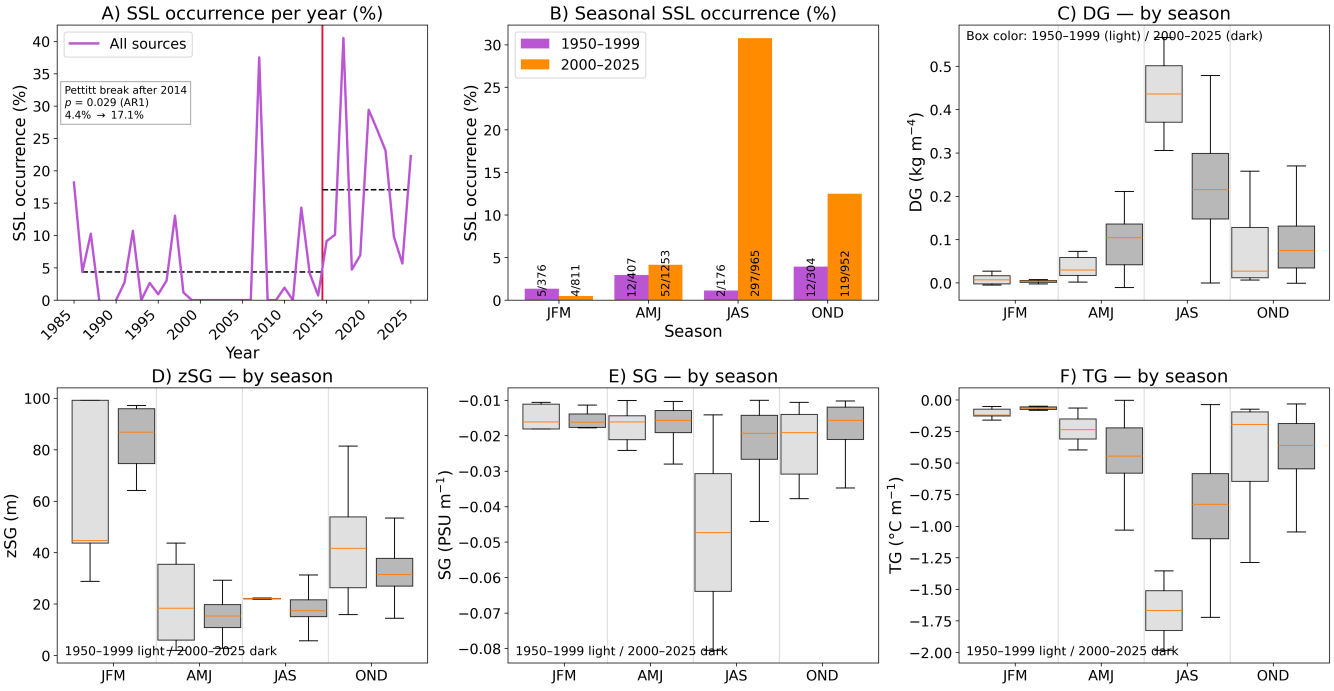


Figure 3. Surface saline lakes in the southern Adriatic, restricted to resolution-matched casts: median level spacing ≤ 5 m and at least 8 levels in 0–100 m, computed per cast from the source profiles. **(A)** Annual occurrence among evaluated casts; the red line marks the Pettitt level shift after 2014 and the dashed lines the means either side. **(B)** Seasonal occurrence by period, annotated with detections over evaluated casts. **(C–F)** Seasonal distributions of the density gradient, core depth, salinity gradient and temperature gradient of the SSL core, for detected events only, light boxes for 1950–1999 and dark for 2000–2025. Restricting to matched casts is essential: at historical bottle spacing the detection criteria return nothing at all (Fig. A1). The 1950–1999 summer boxes in (C–F) rest on the two matched detections of that season and period (panel B) and should not be read as distributions.

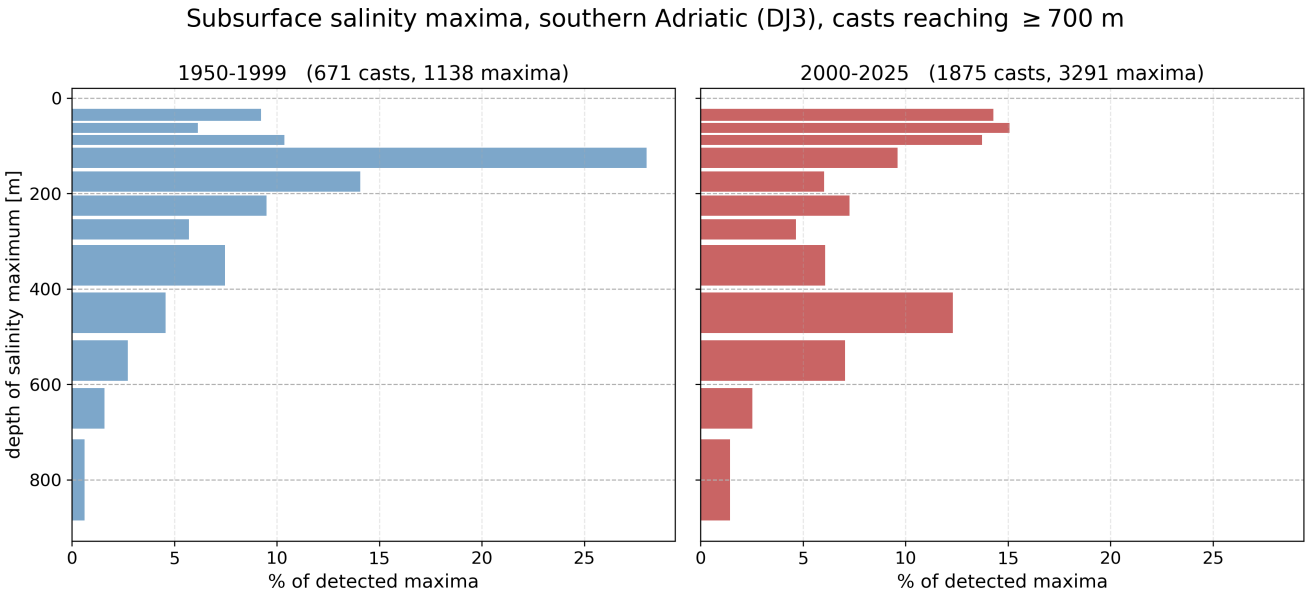


Figure 4. Subsurface salinity maxima in the southern Adriatic, detected individually in each cast by peak prominence, for 1950–1999 and 2000–2025. Only casts reaching 700 m are used, which alone can resolve both features, and only the two most prominent maxima of each cast are retained; a cast carrying a single maximum contributes one detection, which is why the number of maxima is less than twice the number of casts. The cap is needed because at a prominence threshold of 0.010 a small number of very high-resolution historical casts return hundreds of peaks each, and twenty such casts would otherwise supply more than half of all 1950–1999 detections. In 1950–1999 the maxima concentrate in one band, 28 % of them in the single 100–150 m interval and 42 % within 100–200 m; in 2000–2025 that band holds 16 % and the detections are spread through the column, both above 100 m and below 300 m. The historical distribution is what a single-core description of the intermediate layer represents; the modern one is not. Detection is on native vertical resolution; the degraded-resolution repeat is reported in Sect. 3.4. Panels share a common horizontal scale.

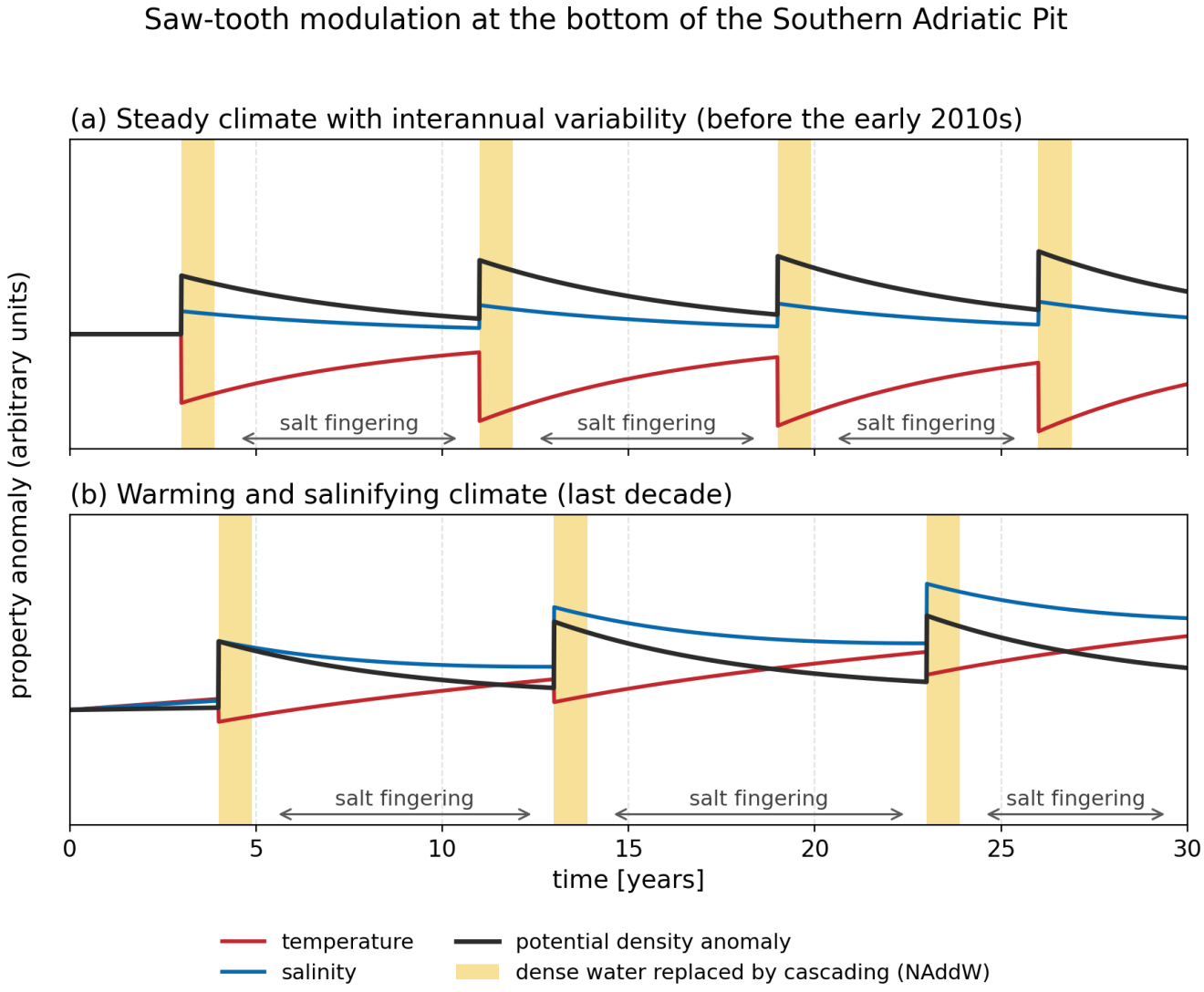


Figure 5. Schematic saw-tooth modulation of temperature, salinity and potential density anomaly at the bottom of the Southern Adriatic Pit. Panel (a) follows the saw-tooth described by Querin et al. (2016); panel (b) sketches how it is modified under the recent regime. **(a)** Steady climate with interannual variability, before the early 2010s: each cascading event delivers cold water, so density rises mainly through the thermal term and properties differ from year to year. **(b)** Warming and salinifying climate of the last decade (Terzić et al., 2025a): cascading water is only weakly cooled but much saltier, so the density step is smaller and the record carries an underlying warming and salinifying drift. Yellow bars mark the intervals during which resident deep water is replaced by cascading North Adriatic Dense Water; between them, properties relax under double-diffusive and other mixing. Salt fingering is marked over the relaxation phases only, and is intermittent because the density ratio rather than the Turner angle governs whether fingers transport appreciably (Sect. 3.7). This is a schematic, not a data plot.

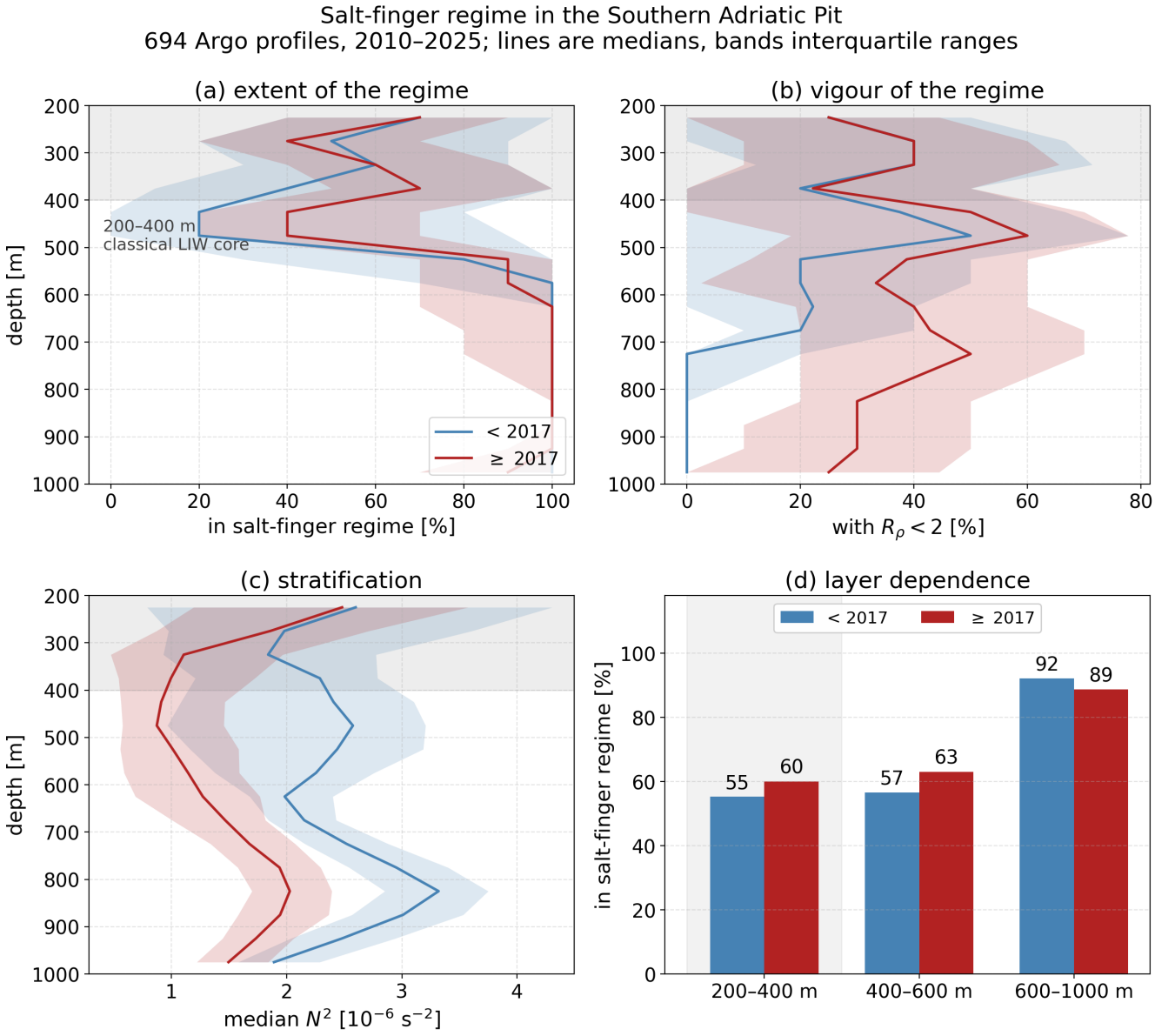


Figure 6. Salt-finger regime in the Southern Adriatic Pit from 694 Argo profiles, 2010–2025, split before and from 2017. Lines are medians across profiles within each 50 m depth bin, bands the interquartile range. **(a)** Fraction of each bin in the salt-finger regime: the extent of the regime. **(b)** Fraction with density ratio $R_\rho < 2$, the range in which fingers grow fast enough to outrun internal-wave strain: the vigour of the regime. **(c)** Median N^2. The grey band marks the classical 200–400 m LIW salinity-maximum range. **(d)** The three layers of Sect. 2.9 compared directly, as the extent of the regime before and from 2017: within the shaded core it does not change significantly (55 % against 60 %, $p = 0.07$), it rises below the core (57 % to 63 % at 400–600 m) and edges down in the deep layer (92 % to 89 %) where the regime is already close to saturation. The vigour of the regime, panel (b), separates the layers far more sharply than the extent does; both are tabulated with their p-values in Table 5.

Appendix A: Supporting analyses

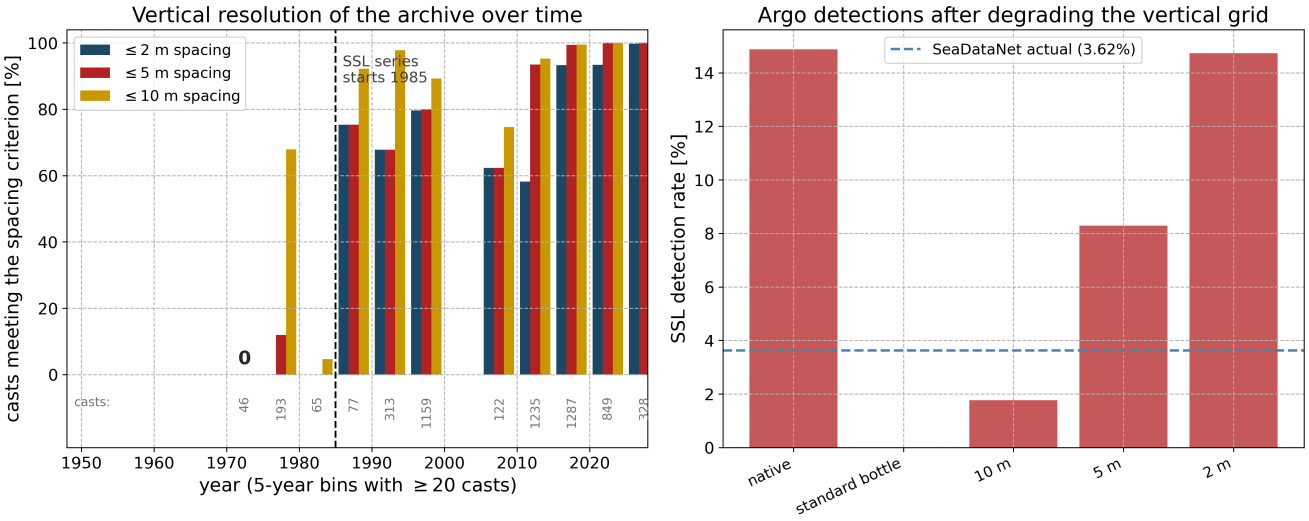


Figure A1. Why surface saline lake occurrence must be read on resolution-matched casts. **Left:** the vertical resolution of the southern Adriatic archive itself, as the percentage of casts per five-year bin whose median level spacing in 0–100 m meets each criterion; bins with fewer than 20 casts are omitted. Bins are labelled with the number of casts behind them, and a bin whose bars are all zero is marked "0", so that an empty bin is not read as missing data. Before 1975 casts exist but none reaches even 10 m median spacing; the 1975–1979 casts are markedly better, 68 % of them at 10 m and 12 % at 5 m, but those fine casts carry too few levels to be evaluated (Sect. 2.6), which is why occurrence is plotted only from 1985 (dashed line). After 2015 almost every cast meets the 5 m criterion used for the gate. **Right:** the degradation experiment. Argo profiles are re-sampled onto progressively coarser vertical grids and the identical detection criteria re-applied. Detections fall from 438 (14.87 %) at native 1–5 m spacing to 434 at 2 m, 244 at 5 m, 52 at 10 m and zero on the standard bottle grid (0, 10, 20, 30, 50, 75, 100 m), in profiles that demonstrably contain a surface saline lake at native resolution; the dashed line is the rate SeaDataNet actually returns at its own resolution. Together these are the justification for the resolution gate applied in Fig. 3.

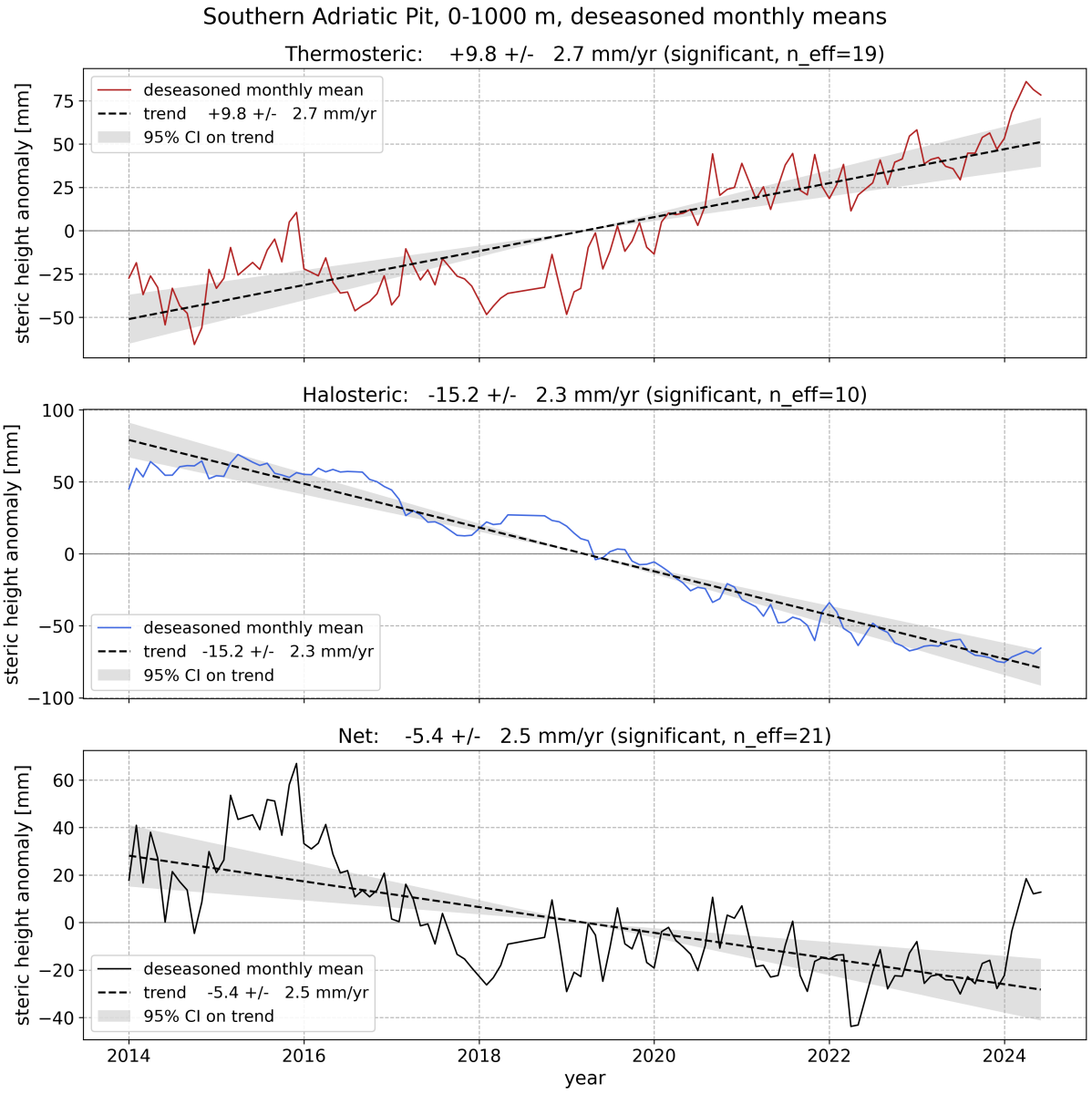


Figure A2. Thermosteric, halosteric and net steric height in the Southern Adriatic Pit over 2014–2024, the window of Table 3, from deseasoned monthly means on a common 0–1000 dbar grid, with fitted trends and 95 % confidence bands corrected for residual autocorrelation. Anomalies are shown about each series mean, so that the three panels are comparable. The window holds 121 monthly values, but successive months resemble one another (lag-1 correlation 0.7–0.8), so the effective sample size $n_{\mathrm{eff}} = n(1-r_1)/(1+r_1)$ behind each interval is only 10–21. The bands are wide for that reason, not because the monthly means are noisy.

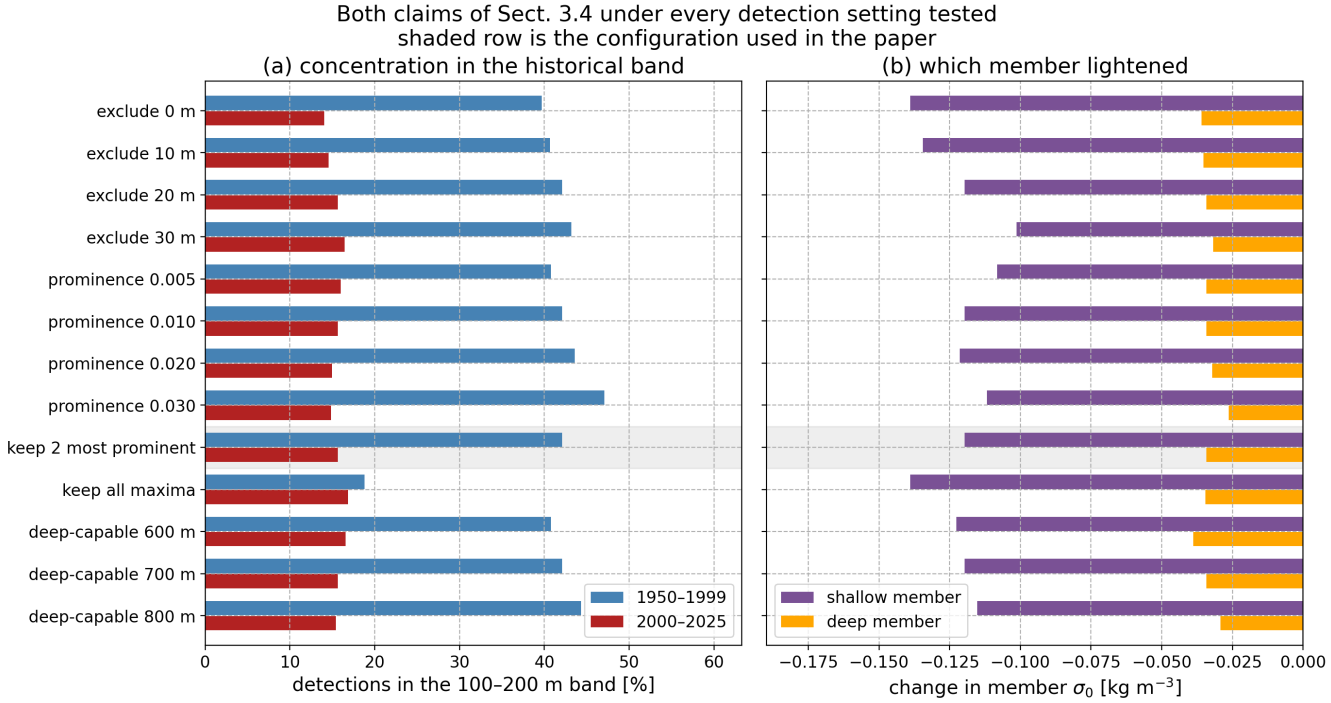


Figure A3. The two claims of Sect. 3.4 under every setting of the detection we tested. The free parameters (Sect. 2.7) are the depth above which maxima are ignored, the prominence threshold, whether all maxima or only the two most prominent are kept per cast, and how deep a cast must reach to be used; each row varies one of them and the shaded row is the configuration used in the paper. **(a)** Share of detected maxima falling in the 100–200 m band. It is higher in 1950–1999 than in 2000–2025 in all thirteen configurations, by 39.7–47.1 % against 14.0–16.9 %. **(b)** Change in σ_0 of each member between the periods. The shallower member lightens by three to four times as much as the deeper one, again in every configuration.